Accepted Manuscript

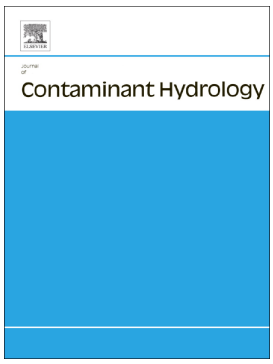

Characterizing the immiscible transport properties of diesel and water in peat soil

Behrad Gharedaghloo, Jonathan S. Price

PII: S0169-7722(18)30229-8
DOI: https://doi.org/10.1016/j.jconhyd.2018.12.005
Reference: CONHYD 3451

To appear in: *Journal of Contaminant Hydrology*

Received date: 26 July 2018
Revised date: 13 November 2018
Accepted date: 19 December 2018

Please cite this article as: Behrad Gharedaghloo, Jonathan S. Price , Characterizing the immiscible transport properties of diesel and water in peat soil. Conhyd (2018), https://doi.org/10.1016/j.jconhyd.2018.12.005

Characterizing the immiscible transport properties of diesel and water in peat soil

Behrad Gharedaghloo[1,2,*] bghareda@uwaterloo.ca, Jonathan S. Price[1] behradg@aquanty.com

[1]Wetlands Hydrology Laboratory, Department of Geography and Environmental Management, University of Waterloo, Waterloo, ON

[2]Currently at Aquanty Inc., Waterloo, ON

[*]Corresponding author.

Abstract

Extensive pipeline and railway corridors crossing Canadian peatlands make them vulnerable to hydrocarbon spills, potentially impairing ecosystem health, so it is important to be able to forecast hydrocarbon fate and transport within and beyond the peatland. The redistribution of hydrocarbon liquids in groundwater systems are controlled by the multiphase flow characteristics of the aquifer material including capillary pressure-saturation-relative permeability (P_c-S-k_r) relations. However, these relations have never been characterized for the hydrocarbon-water phases in peat. To address this, the flow and transport of diesel and water in peat soils were examined through a number of one dimensional vertical immiscible displacement tests, in which diesel was percolated into peat pore space displacing peat water, leading to a two-phase flow regime. Inverse modelling simulations using both Brooks and Corey's and power law relative permeability models, matched the data of the immiscible displacement tests well. Irreducible water saturation (S_{wirr}) and the curvature of water relative permeability relation increased with peat bulk density. The residual diesel saturation (S_{Nr}) ranged between 0.3-17% and increased with bulk density of peat. In a given peat, S_{Nr} was a function of saturation history and increased with increasing maximum diesel saturation. The receding contact angles of water in water-air systems and diesel in diesel-air systems, respectively, were 51.7° and 61.2°, showing that the wetting tendency of peat in the air imbibition condition is toward the draining liquid. These experiments

advance our knowledge on the behavior of hydrocarbons in peat, and can improve numerical modelling of hydrocarbon transport after a spill.

Keywords: NAPL spill; multiphase flow; residual NAPL saturation; peat; relative permeability; contact angle

1. Introduction

After a hydrocarbon spill onto a peatland, the hydrocarbon as a light non-aqueous phase liquid (NAPL) will spread in the aquifer and contaminate the down-gradient ecosystem. NAPL spreading velocity and extent in the contaminated aquifer will be controlled by multiphase flow properties of the aquifer material, including capillary pressure-saturation-relative permeability relations (P_c-S-k_r). The spatial distribution of the NAPL plume controls the rate of volatilization, as well as dissolution of organic molecules in water, and determines the spatial distributions and temporal variations of dissolved contaminants down-gradient of the spill zone. Ideally, environmental scientists could forecast the distribution of the NAPL plume, but given the poor understanding of multiphase flow in peat, and the absence of parameters characterizing it, this cannot currently be done.

The P_c-S-k_r relation has been characterized for glass beads (e.g. Johnson et al. 1959), unconsolidated sand (e.g. Leverett and Lewis 1941) and sandstones (e.g. Caudle et al. 1951), but not for peat soils. Among the parameters of P_c-S-k_r relations, residual NAPL saturation (S_{Nr}) dominantly controls the extent of the free-phase plume. S_{Nr} is the NAPL saturation in which the relative permeability of NAPL, and consequently its mobility, tends to zero and NAPL stops moving. For a given volume of spilled NAPL, the higher the S_{Nr}, the smaller will be the final extent of a free-phase plume. In downward percolation of spilled NAPL, the magnitude of S_{Nr} determines the mass of NAPL left in the vadose zone and whether free NAPL reaches water table or not. This parameter has not been characterized in peat soils.

After reaching the water table (WT), Light NAPL (LNAPL) spreads above the water table and moves laterally down-gradient. In addition, WT fluctuations can displace the LNAPL (Oostrom et al. 2006) and enhance the lateral extent of the free-phase plume. The WT fluctuations could be frequent in peatlands due to the shallow WT in these aquifers where the thin unsaturated zone has little capacity to buffer against atmospheric water fluxes. Related observations on the magnitude of the lateral migration of LNAPL above the WT and the effect of WT fluctuations on NAPL redistribution have thus far not been documented for peatlands.

Although P_c-S-k_r relations have not been characterized for NAPL-water system in peat, they have been measured frequently for air-water system (e.g., Price et al. 2008; Price and Whittington 2010; McCarter and Price 2014). Due to the lower complexity of air-water measurements compared to NAPL-water measurements, as well as availability of P_c-S-k_r data of air-water systems, using air-water measurements to estimate NAPL-water relations could reduce the cost and characterization time. Notwithstanding the lack of a comparison between air-water and NAPL-water relations in peat soils, a comparison could indicate the similarities and differences and if air-water data are a reasonable proxy for NAPL-water simulations.

The aim of this study is 1) to characterize P_c-S-k_r relations and the residual NAPL saturation in peat soils in varying spill scenarios; 2) to observe the magnitude of the downward and lateral migration of LNAPL above the WT, and to examine the effect of WT fluctuations on NAPL redistribution; and 3) to compare P_c-S-k_r data of a water-NAPL system to those available for air-water systems, and to assess if air-water data provide reasonable estimates of NAPL-water relations. To fit this purpose, one-dimensional and two-dimensional peat column experiments were carried out. In these experiments, diesel was used as the NAPL, since it is a common petroleum product that is transported via pipelines and railroads. In the case of a diesel spill onto a peatland, in addition to release of free-phase and dissolved-phase hydrocarbon contaminants, it might remobilize non-organic contaminants such as lead, in peatlands (Deiss et al. 2004). The results of this study will help groundwater modellers and environmental scientists evaluate the behavior of petroleum hydrocarbon contaminants in peatlands and assess the risk of contamination.

2. Methods

2.1. Contact angle and scaling capillary pressure relations

Air-water capillary pressure-saturation (P_c-S) relations have frequently been characterized and reported for different types of peat soils (Schwärzel et al. 2006; Price et al. 2008; McCarter et al. 2014) and could be used for a NAPL-contaminated peatland if they can be scaled to NAPL-air and NAPL-water systems. Several studies have scaled P_c-S data between liquid-liquid and liquid-gas systems (e.g., Parker et al. 1987; Lenhard and Parker 1988). Scaling these data and relations requires knowledge of the interfacial tensions and contact angles of fluids present in the pore space (Demond and Roberts 1991; Bradford and Leij 1995a). To investigate the validity of scaling in peat, corresponding P_c-S data and contact angles for different fluid combinations were measured. To measure the contact angles, air bubbles were released onto a peat surface in water or diesel saturated conditions, then the geometry of the bubbles (Figure 1) were analyzed to determine the contact angles. Details are available in Gharedaghloo and Price (2017), who showed contact angle of water-NAPL system in water drainage and NAPL drainage conditions. Here, we report the contact angles of water-air, and NAPL-air (diesel-air) systems, for the condition of air imbibition (water drainage and diesel drainage).

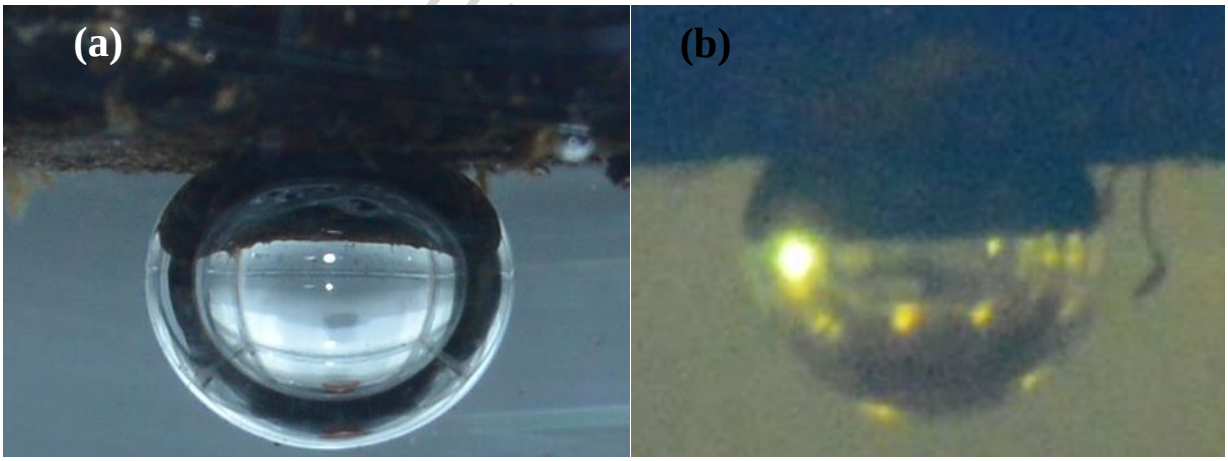

Figure 1: Air bubble on peat in the water saturated condition (a), and diesel saturated condition (b), illustrating the water-air and diesel-air contact angles in gas imbibition, respectively.

To obtain the capillary pressure-saturation relations in peat soil in a controlled and reproducible condition, gravity drainage column tests were carried out using milled peat. Milled peat was screened with 1 mm sieve to decrease the heterogeneities and to ascertain that peat particles are of similar size, so the pore size distributions between columns were similar. A column (Figure 2a) with separable segments was filled with milled peat. The dimensions of each segment were 5 cm length and 10 cm internal diameter. The peat in each segment was packed individually and with a given dry peat weight, before inserting into the column; this was done to seek homogeneous bulk density, porosity, and pore size distribution along each column and between replicates. The packed peat column then was saturated with the desired liquid (water or diesel) in the upward direction through the bottom of the column to minimize air trapping. After saturation, the column was drained by opening its bottom valve leading to liquid drainage through bottom of the soil column and air imbibition through the top (Figure 2a). After 48 hours of drainage when the outflowing rate was zero the column was separated into segments starting from the top. The weight of a drained segment and the original dry weight of milled peat then were used to calculate the volume and the saturation of the liquid (water or diesel) in the segment. Repeating this for all segments, the variation of liquid saturation with height (Figure 2b) was obtained. The procedure was repeated in 3 replicates for water drainage and in 2 replicates for diesel drainage.

Next, the diesel-air data were scaled and compared to water-air data using Equation 1, where σ_{aw} is air-water interfacial tension, σ_{ad} is air-diesel interfacial tension, θ_{aw} is water contact angle at the air-water interface on peat surface, θ_{ad} is diesel contact angle at air-diesel interface on peat surface, P_{cad} is capillary pressure in the diesel-air system at diesel saturation of S_d, and P_{caw} is capillary pressure in the water-air system at water saturation of S_w. In scaling, σ_{da} and σ_{wa}, respectively, were considered as 23.8 mN/m (Environment Canada 2018) and 72.0 mN/m (Lide 2012); the median diesel-air and water-air contact angles obtained in contact angle measurements were used in the scaling.

$$P_{caw}(S_w) = \frac{\sigma_{aw}\cos(\theta_{aw})}{\sigma_{ad}\cos(\theta_{ad})} P_{cad}(S_d) \qquad \textbf{Equation 1}$$

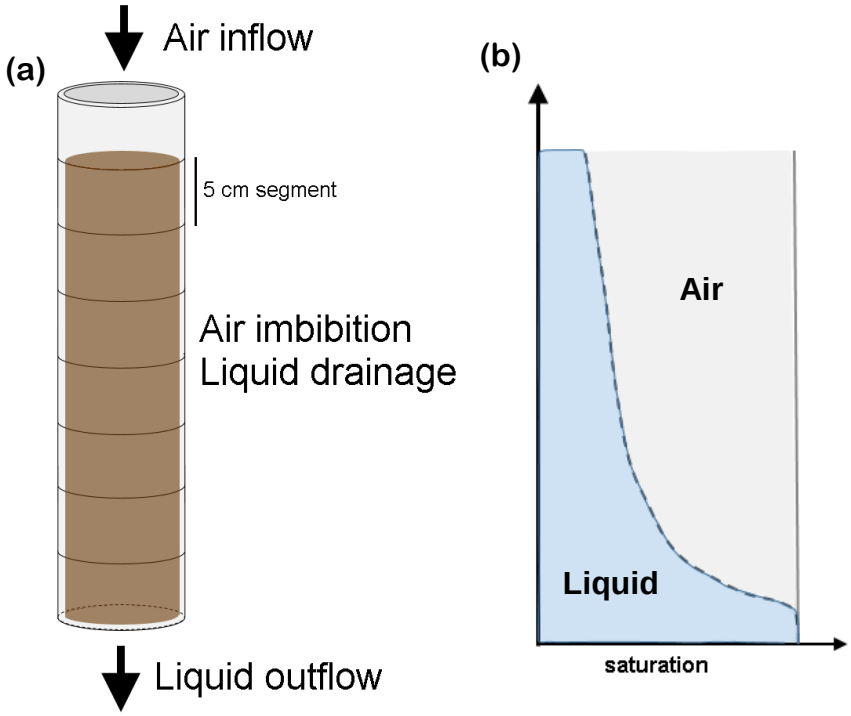

Figure 2: Air inflow through top and liquid outflow through bottom of the separable column causing liquid drainage and air imbibition along the soil column (a); idealized vertical distributions of liquid and air saturation along the column at the end of the experiment (b).

2.2. Unsteady state displacement column test

One dimensional studies of NAPL percolation into vertical soil columns (e.g. Lenhard et al. 1988; Thomson et al. 1992) have been carried out to assess the behavior of NAPL during imbibition into the soil pore. In addition, such vertical columns have been used to determine the relative permeability relations (Sahni et al. 1998; DiCarlo et al. 2000) and NAPL recovery (e.g. Kantzas et al. 1988) under gravity drainage conditions. Such vertical displacement tests could be representative of the condition of NAPL spilled on a water saturated soil surface (e.g. in a train derailment), after which NAPL spreads above the peat surface and percolates downward into the soil profile due to water table drawdown. This mimics the conditions of a spill accident following snowmelt or other wet periods of the year, when the water table is at or above the ground surface. Unsteady-state immiscible displacement tests were carried out in (unsegmented) vertical peat

columns. The aim was to simulate the percolation of NAPL into the peat profile, to indicate the effects of peat properties on NAPL percolation rate and NAPL trapping, and to quantify k_r of the diesel phase in peat columns under the gravity drainage condition.

Two types of peat (A and B) with different physical properties were used in these experiments. Peat A was extracted from a bog peatland in Quebec (47° 58' N, 69° 26' W) and peat B was from a bog peatland in Southern Ontario (43° 55' N, 80° 25' W), and the extracted peat monoliths were frozen after extraction. The top of each peat monolith was at the ground surface (top of surface moss layer) and the lengths of the monoliths were ~40 cm, providing a peat profile between the ground surface down to ~40 cm below ground surface. From each frozen peat monolith (peat A and B) three columns (A1, A2, A3, B1, B2, B3) with diameter of 5.1 cm and length between 30-36 cm were cut; one compacted peat column (A4) was also made using residue of peat A. The aim of using a compacted column was to compare the results of a highly disturbed (compacted) column and the intact columns. Each column was first saturated from the bottom with deionized water to minimize air trapping. Constant head permeability tests were carried out with deionized water on the columns to obtain their hydraulic conductivity and absolute permeability.

Next, a 17.6-25.3 cm diesel column (varying between columns) was placed at the surface of water-saturated peat (Figure 3a). The bottom valve of the column was then opened allowing water to flow out the column and diesel to imbibe into it due to gravity (Figure 3b). Through diesel imbibition, diesel head above the peat surface declined continuously and equaled zero when the diesel-table was at the peat surface (Figure 3c) after which two-phase flow of diesel-water ended and air started imbibing into the pore space, forming a three-phase flow regime along the soil column. During the experiment the cumulative produced volumes of water and diesel were recorded for the two phase flow period and a part of the three-phase flow period (Figure 3d) to be used in relative permeability calculations. Gravity drainage continued for ~48 hours until water and diesel outflow ceased. No change in the height of compressible peat columns was observed during the experiment.

In all columns of peat A, diesel breakthrough occurred before the two-phase flow period ended. However, diesel breakthrough at the outflow did not occur in column B1 at the end of the two-phase flow period, thus the diesel production trend was not recorded for this core. Again, for

column B2, the initial height of diesel column was not sufficient to cause diesel breakthrough by the time the diesel level declined to the peat surface; so in this column, diesel was added gradually to the peat surface to maintain the diesel head at the peat surface and delay air imbibition until diesel production at the outflow started and continued for few minutes. To avoid such discrepancies, in column B3, the initial height of diesel column was increased to 25.3 cm to ascertain diesel breakthrough and its production at the end of two-phase flow period of the experiment.

At the end of the gravity drainage process, to determine the final distributions of water and diesel along the columns, each column was cut into ~5 cm segments, and the segments were squeezed with a hydraulic press (~120 atm) to extract the water and diesel. The deformable peat matrix provided good water and NAPL recovery from its pore spaces. However, since not all fluids were recovered by pressing, in-situ residual volumes and saturations of water and diesel were estimated (Appendix A) based on the extracted volumes of water and diesel and the air-dried weight of the peat. The air-dried weight was also used to calculate bulk density and porosity. Finally, the balance of residual diesel volume in peat columns was checked (Appendix B) to ascertain that no significant error was imposed.

The relative permeability of peat to diesel (kr_D) was estimated using the cumulative diesel percolation and production data. Diesel breakthrough at the column outflow indicated a continuous diesel phase along the column, which means the average relative permeability of diesel in the column could be calculated using diesel head data and its outflow rate. If at two times, t_1 and t_2 [T] diesel heads are h_1 and h_2 [L], respectively, and the average diesel outflow rate between t_1 and t_2 is Q_D [L^3T^{-1}], the average effective hydraulic conductivity of diesel (K_{effD}) between t_1 and t_2 is estimated using Darcy's law (Equation 2) for diesel such that

Equation 2

$$K_{effD} = \frac{Q_D L}{A \Delta h}$$

where A is cross sectional area of the peat column [L^2], L is the length of the column [L], and Δh is the head difference between up-gradient (top of peat column) and down-gradient (bottom of peat

column) [L], which is equal to (h_1+h_2)/2. Next, effective permeability of peat to diesel (k_{effD}) was obtained using

Equation 3

$$k_{effD} = \frac{K_{effD}\mu_D}{\rho_D g}$$

where μ_D is diesel viscosity [$MT^{-1}L^{-1}$], ρ_D is diesel density [ML^{-3}], and g is acceleration constant [LT^{-2}]. Finally, kr_D was calculated as the ratio of k_{effD} and absolute permeability (k) of the peat column. The average water saturation (S_w) along the column between t_1 and t_2 was obtained using the cumulative water production data. If cumulative produced water volumes at t_1 and t_2 are V_{w1} and V_{w2}, the average cumulative water production between t_1 and t_2 ((V_{w1}+V_{w2})/2) demonstrates the drained volume, thus the drained porosity. Using the drained porosity and the total porosity of column, the average water saturation between t_1 and t_2 was calculated. Repeating these for every two adjacent measurements, the variations of diesel relative permeability with water saturation were obtained for each tested column. This relative permeability of diesel is for the water drainage condition.

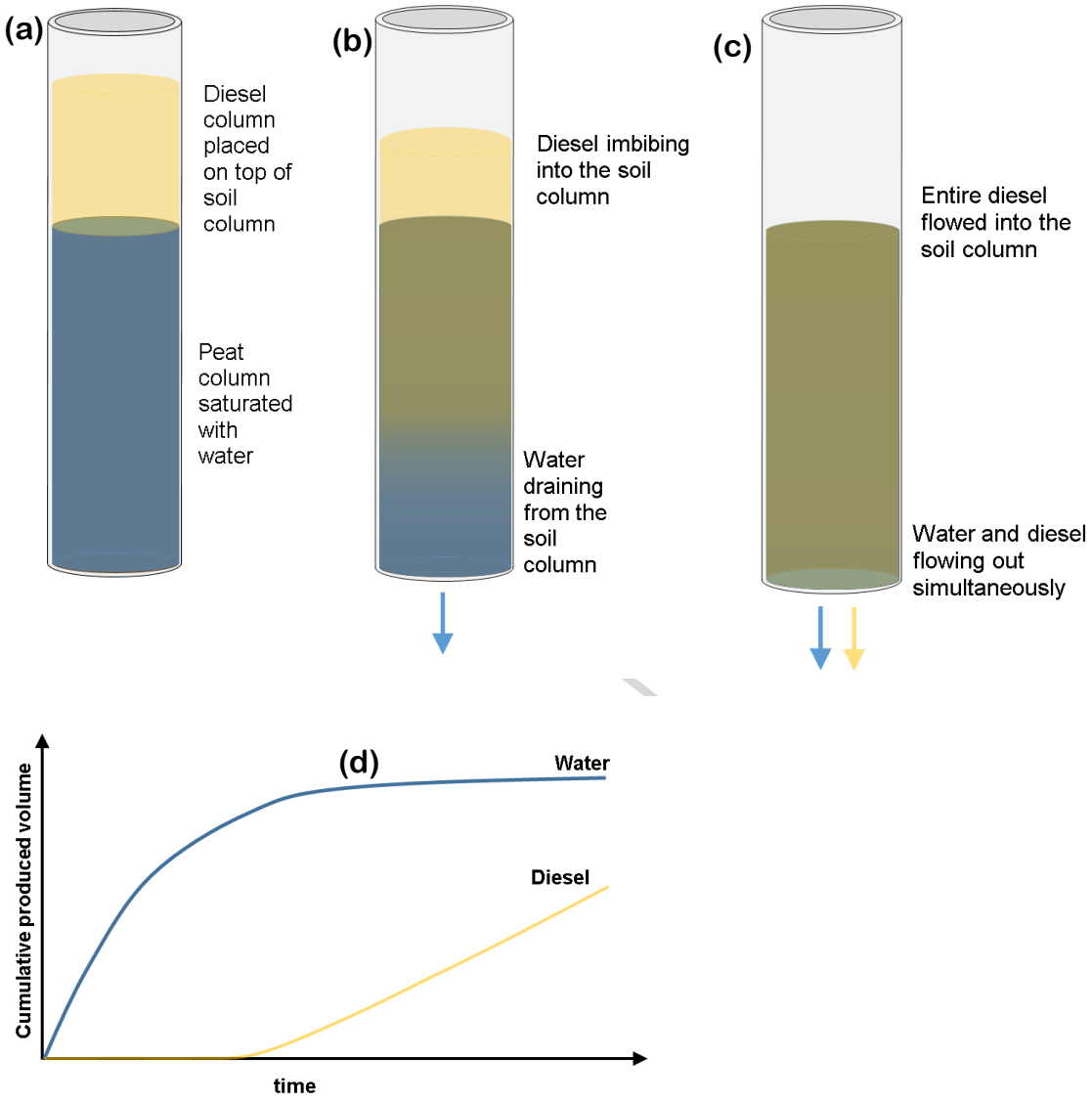

Figure 3: (a) peat column is saturated with water and a diesel head is placed above the peat surface; (b) outflow valve is opened, diesel imbibes into the soil column and water flows out through column bottom due to gravity drainage; (c) three-phase flow begins when no diesel head is left above soil surface; (d) idealized variations of cumulative produced water and diesel through the two-phase flow period of the experiment

2.3. Inverse modelling and estimating P_c-S-k_r functions

Capillary pressure and relative permeability functions have been estimated through inverse modelling in NAPL-water and air-water system (Chardaire-Riviere et al. 1992; Sigmund and

McCaffery 1979; O'Carroll et al. 2005; Parker et al. 1985; Crescimanno and Iovino 1995). In these studies, P_c-S-k_r functions of porous media were treated as fitting parameters and were adjusted to match observed data with numerical simulation results. In a similar approach, here, the two-phase flow periods of the immiscible displacement tests were used to estimate P_c-S-k_r functions of peat. The aim was to match the measured water and diesel cumulative outflows with a numerical model through adjusting peat P_c-S-k_r functions. Two different forms of P_c-S-k_r relations were used: 1) the Brooks and Corey's (1964) model, and 2) power law model (PLM) with no capillary pressure. Equation 4 to Equation 7 describe the P_c-S-k_r functions of Brooks and Corey's model (BCM) where P_{cth} is the threshold capillary pressure at which water drainage begins and diesel starts imbibing into the largest pore sizes corresponding to P_{cth}, S_e is the normalized water saturation, S_w is water saturation, S_{wirr} is the irreducible water saturation and is the water saturation at which water ceases flowing, λ is pore size distribution factor of the porous medium, k_{rw} is water relative permeability and k_{rN} is diesel (NAPL) relative permeability. λ controls the curvature of the k_r-S curves.

$$P_c = P_{cth} S_e^{-1/\lambda} \quad \textbf{Equation 4}$$

$$S_e = \frac{S_w - S_{wirr}}{1 - S_{wirr}} \quad \textbf{Equation 5}$$

$$k_{rw} = S_e^{\frac{2+3\lambda}{\lambda}} \quad \textbf{Equation 6}$$

$$k_{rN} = (1 - S_e)^2 \left(1 - S_e^{2+\lambda/\lambda}\right) \quad \textbf{Equation 7}$$

Equation 8 and Equation 9 describe the power law relative permeability relations, in which n_N and n_w, respectively, are the powers of diesel relative permeability and water relative permeability relations and determine the curvature of the relative permeability relations.

$$k_{rw} = S_e^{n_w} \quad \textbf{Equation 8}$$

$$k_{rN} = (1 - S_e)^{n_N} \quad \textbf{Equation 9}$$

To model the two-phase flow of water and NAPL in peat columns, the open-source MATLAB Reservoir Simulation Toolbox (MRST, 2017a) (Lie, 2016) was used. MRST solves the two-phase flow equation (Equation 10) simultaneously for water and diesel, and calculates spatial distribution and temporal variations of saturations and fluxes along the peat columns.

$$\phi\rho_f \frac{\partial S_f}{\partial t} = \frac{\partial}{\partial z}\left(\rho_f \frac{kk_{rf}}{\mu_f}\left(\frac{\partial p_f}{\partial z} - \rho_f g\right)\right) + q_f \qquad \textbf{Equation 10}$$

In Equation 10, *f* is a pore fluid and represents water and diesel phases, S_f is the saturation of the fluid, p_f is the pressure of the fluid [$ML^{-1}T^{-2}$], k_{rf} is the relative permeability of the fluid, $\boldsymbol{k}$ is absolute permeability of peat [L^2], ϕ is porosity, ρ_f is density of the fluid [ML^{-3}], g is gravitational constant [LT^{-2}], z is the elevation [L] and q_f is a sink/source term [$ML^{-3}T^{-1}$]. A one-dimensional vertical model of each column with its corresponding permeability and porosity values was built in MRST. The upper boundary condition of the column was controlled by an imaginary diesel injection well in which the diesel injection rate (as the diesel percolation rate) varied with time. Having the variations of diesel head with time, the temporal variations of diesel rate in the injection cell was obtained.. The boundary condition at the bottom of the column was a production well which operated with atmospheric bottom hole pressure (BHP) and was open to produce both water and diesel. Using the model the outflowing rates of water and diesel at each column's outflow were simulated. The density of diesel was measured as 0.83 g/cm^3 and was used as input in the numerical models. Water density was assumed as $1g/cm^3$ and its dynamic viscosity was assigned as 1 mPa.s. The dynamic viscosity of diesel was assumed as 2 mPa.s at the laboratory condition (Environment Canada, 2018).

Two sets of estimating simulations, one with BCM and the other with PLM, were run for each column. In the estimating simulations with BCM, λ, S_{wirr}, and P_{cth} parameters were treated as the unknown parameters, and in the simulations with PLM, S_{wirr}, n_w, and n_N were the unknown parameters. For each column, MRST simulated the downward percolation of diesel into the peat column and calculated the variations water and diesel outflowing rates with time. Next the root-mean-square-error (*RMSE*) of diesel cumulative outflowing volume was calculated with

$$RMSE = \sqrt{\frac{\sum_{i=1}^{n}\left(y_i^{measured} - y_i^{simulated}\right)^2}{n}} \qquad \textbf{Equation 11}$$

where n is number of observed points, $y_i^{measured}$ is a value of observed cumulative diesel volume and $y_i^{simulated}$ is the corresponding value at in the simulated case. FMINCON minimizing function of MATLAB was used to minimize *RMSE* through adjusting and calibrating the unknown parameters. Finally, the realization with the lowest *RMSE* was selected as the model with representative model parameters.

Studies have raised concerns regarding uniqueness of the results obtained by this method (Kool et al. 1985; Eching and Hopmans 1993) meaning that there is a possibility that two or more sets of P_c-S-k_r data result in similar minimum objective functions. Eching and Hopmans (1993) recommended measuring pressure in the core to resolve the non-uniqueness issue; however there are other arguments that the including tensiometer data in inverse modelling are not necessary (O'Carroll et al. 2005). To avoid the possible problem of non-uniqueness, the calculated k_r-S data of diesel (discussed in previous section) was another check-point for the estimated diesel k_r-S relations.

2.4. Diesel spill in a two dimensional peat box model

Two-dimensional experimental soil boxes have been used to study the redistribution of NAPL in porous material (Høst-Madsen and Jensen 1992), the effect of water table variations on the behavior of NAPL (Oostrom et al. 2006), the effect of soil heterogeneity on NAPL redistribution (Illangasekare et al. 1995), and the recovery of petroleum contaminants through flooding them (Palomino and Grubb 2004). These 2-D box models allow control of the environmental condition and release of hydrocarbon between field-scale and core-scale studies. Using these box models, the redistribution of NAPLs can be studied where releasing a field-scale spill is not an option. Here, the peat box model was used to observe the redistribution of diesel in vadose zone of peat and to evaluate the effect of water table fluctuations on its remobilization. This experiment mimics the condition where the water table is deep and diesel is spilled on the surface of peat vadose zone.

An intact peat sample (50 cm x 50cm x 10 cm) was extracted from peatland B. Extraction was done in winter when the top 30 cm of the soil was frozen to minimize monolith disturbance. The top of the extracted peat monolith was the ground surface, and it covered the peat profile down to 50 cm below ground surface. The peat monolith was placed in the main chamber of a peat box (Figure 4). A "well" at each side of the box connected to the main chamber with screens allowed adjustment of the water table (WT) and visual monitoring of WT and free diesel thickness in the peat box during the experiment. At the field scale the wells could represent ditches excavated around the spill area to collect spilled liquids.

Monitoring NAPL percolation and spreading in pore spaces in laboratory-scale studies has been done visually (e.g. Van Geel and Sykes 1994; Darnault et al. 1998; Palomino and Grubb 2004; Conrad et al. 2002), using X-ray (e.g. Fagerlund and 2007; Goldstein et al. 2007), dual gamma attenuation (e.g. Høst-Madsen and Jensen 1992), and electrical resistance (e.g. Pantazidou and Sitar 1993). Measuring the electrical resistance of porous media has been a tool for characterizing the variations of aqueous phase saturations in pore space in other earlier studies (e.g. Leverett 1939; Leverett and Lewis 1941; Morgan and Pirson 1964). The peat box was equipped with electrical resistivity sensors intended to monitor NAPL percolation during and following the diesel spill. To accomplish this the peat column was flushed with 50 litres of 100 mg/L sodium chloride solution for 2 weeks before the spill to place an electrically conductive aqueous fluid in peat pore space. A network of electrodes were embedded at the front and back of the 2D column (Figure 4). At the end of brine flushing, the WT level was set at 9.5 cm above the bottom of the peat (~40 cm below ground surface). The WT then was monitored over the following 4 days to ascertain physical equilibrium established between air and water phases before the spill.

A network of 8 hydrophilic and 8 hydrophobic pressure transducers were embedded at the front face of the peat box (Figure 4) to measure water and diesel pressures, respectively, during the experiment. Preparation and treatment of the transducers are discussed in Appendix C. Primary measurements showed that the response time of a transducer was ~10 minutes which was not short enough to allow fluid pressures measurement with sufficient frequency during and following the spill. However, the transducers allowed monitoring of the temporal variations of water pressure before the spill, and water and diesel pressures after the spill. This helped us to decide whether

physical equilibrium was established between pore fluids, before and after spill, and following the rainfall events and water table fluctuations. Before and after each event, the pressure values were monitored; the absence of temporal variations of pressure during these periods in all the transducers was assumed to imply physical equilibrium.

To simulate the spill, diesel was released via a mesh of tubes that were uniformly distributing the diesel at a constant rate of 17.7 mL/min over the central 20 cm of the peat box (area of 200 cm^2). The diesel spill continued for 105 minutes, cumulatively releasing 1858 mL of diesel to the peat surface. The thickness of free NAPL above the WT at the side well and within the peat box was monitored following the spill. Starting 7 days after the spill, diesel was pumped out from the side wells. This was to simulate the lateral redistribution of NAPL in a field condition, to the surrounding area or to excavated ditches. NAPL was collected over the next 2 weeks until no free NAPL was evident at the side wells. The aim was to encourage lateral migration until the remaining free-phase diesel in pore spaces reached residual saturation, thus no further movement.

Next, two heavy rainfall events were simulated by releasing drips of deionized water across the peat surface via a network of tubes with 2.5 cm spacing. The aim of the simulated rainfall was to raise WT in the peat box so we could observe the effect of WT fluctuations on diesel redistribution. For the first event the rate of water release was 34.7 mL/min, simulating a rainfall event with intensity of 4.2 cm/hour. WT level rose after the rainfall, and the system equilibrated in 24 hours, after which water was removed from the side wells to return WT to the pre-rainfall level. Another rainfall simulation with an intensity of 33.4 mL/min was done, and after 24 h WT was again returned to the pre-rainfall level. NAPL released after each rainfall event was collected from side wells. After the second rainfall the system was monitored for 1 week for possible flow of NAPL to the side wells and to ensure that the system had reached equilibrium. The simulated diesel spill and heavy rainfalls did not impose physical deformations to the compressible peat block of the experiment. The spilled and collected volumes of NAPL and water in the abovementioned events were different. Also, the outflow rates of water and NAPL from the peat column were not similar between the events. That is, the equilibrium time between events was variable.

To determine the spatial distributions of NAPL after these experiments, the peat monolith was cut into segments. To avoid fluid loss during cutting, WT was lowered to the bottom of the peat prior to its removal, so that the fluids were under capillary pressure and would not leak out. The peat monolith was segmented into 25 10×10×10 cm cubes, which were then squeezed with a hydraulic press to collect the remaining diesel and water.

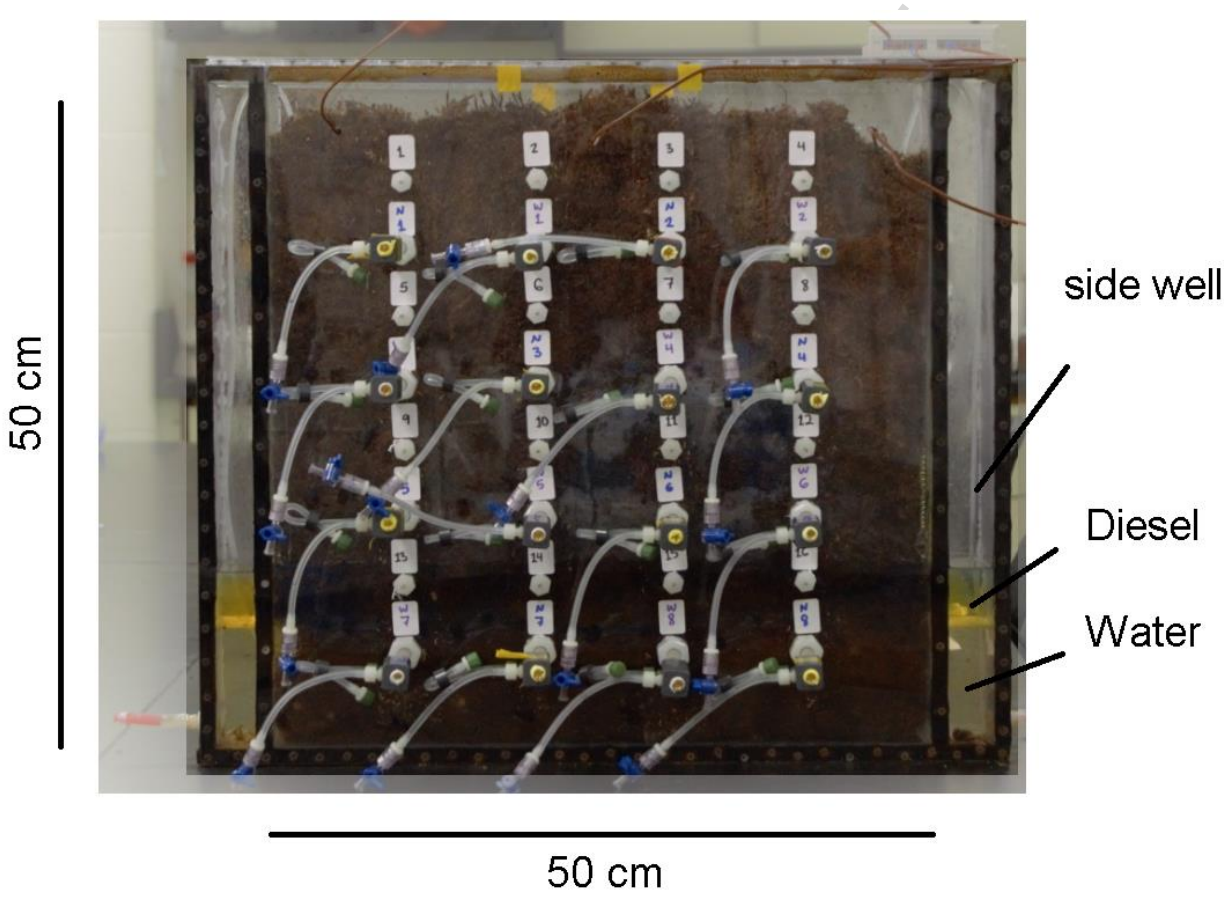

Figure 4: 2D peat box after the diesel spill; side well with diesel and water levels are evident; water and diesel pressure transducers with 10 cm spacing labelled N (for diesel) and W (for water). Hexagonal ports held electrodes enabling electrical resistance measurements through the experiment.

3. Results

3.1. Contact angle and air-liquid column tests

Respectively, 22 and 19 images were processed for water-air and diesel-air contact angles on peat. Water-air contact angles ranged from 39.7°-59.8° with a median of 51.7° (Mean ± St.

dev.=51.6° ± 4.5°). The diesel-air contact angles ranged from 45.9°-73.7° with a median of 61.2° (Mean ± St. dev.=60.2° ± 7.6°). The measured contact angles are specific to saturated conditions and the angle for peat that is partially saturated with water or diesel might be different.

The median values of water and diesel contact angles were used in Equation 1 and in scaling the height-saturation data of the diesel to water-air system. Figure 5a illustrates the elevation-saturation data for the diesel-air and water-air (segmented) column tests, showing that at a given height above the water table or diesel table (pressure=1 atm) the saturation of diesel is evidently less than water saturation (in the presence of air, hydrocarbon retention is less than water retention). In Figure 5b, capillary pressure-saturation data are calculated by converting the elevation to capillary pressure. Then, the capillary pressure-saturation data of the diesel-air system is scaled to that of the water-air system using Equation 1 (Figure 5c).

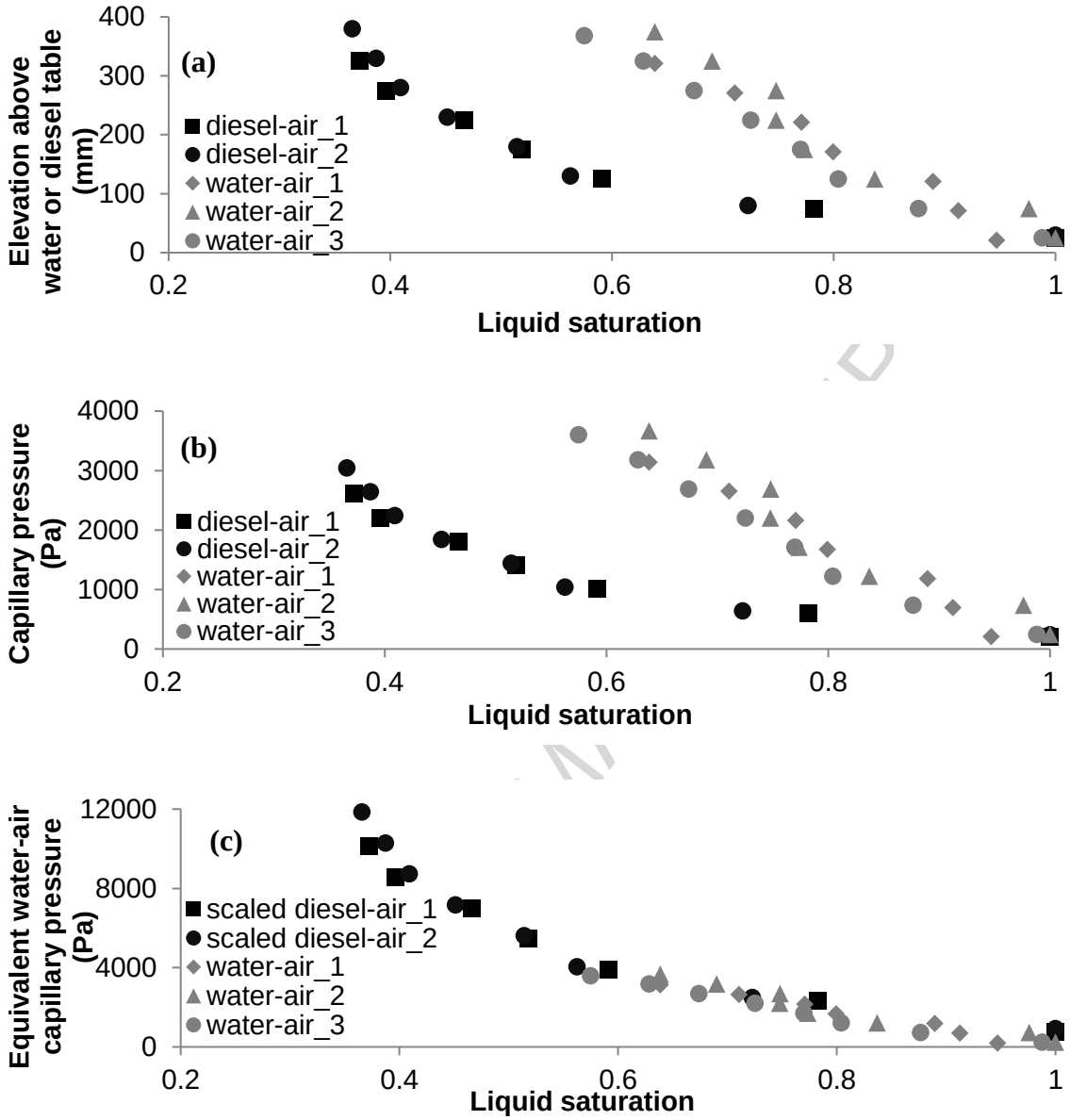

Figure 5: (a) unscaled height-saturation data for diesel-air and water-air column tests using milled peat; (b) unscaled capillary pressure-saturation relations for diesel-air and water-air drainage condition; (c) scaled diesel-air capillary pressure-saturation data (using Equation 1) compared to water-air capillary pressure-saturation data.

3.2. Vertical distributions of diesel and water

The bulk density of the replicates of peat A were between 0.066 to 0.090 g/cm^3, while the bulk for peat B were between 0.026 to 0.035 g/cm^3. Accordingly, the porosity of peat A was less than

that of peat B in the 1D immiscible displacement columns (Table 1). The saturated hydraulic conductivity of peat A ranged from 5.6×10^{-5} m/s to 1.1×10^{-4} m/s (Table 1). The saturated hydraulic conductivity of peat B in this study ranged from 3.5×10^{-4} m/s to 6.4×10^{-4} m/s (Table 1). The average hydraulic conductivity of column A1 to A3 was 8.9×10^{-5} m/s (with standard deviation of 2.9×10^{-5} m/s). On the other hand, the average hydraulic conductivity of columns B1 to B3 was 4.6×10^{-4} m/s (with standard deviation of 1.6×10^{-4} m/s). Thus, the average hydraulic conductivity of peat B was 5.2 times of that of peat A.

The spatial variations of water and liquid (water+diesel) saturations along the columns at the end of immiscible displacement column experiments (Figure 6) show that due to capillarity, liquid and water saturations generally decreased with elevation above bottom of the columns; the increase is more evident in columns of peat A. The average water saturation remaining in columns of peat A is more than the average water saturation of the columns of peat B. In Figure 6, the area between water and liquid saturation curves corresponds to the diesel saturation, showing that average diesel saturation along peat B is less than half that in peat A (Table 1). This shows that residual diesel saturation in peat pore space is inversely correlated with its porosity and hydraulic conductivity and increases with peat bulk density. The results also show that although the peat column was compacted and highly disturbed in A4, its porosity, permeability, and residual diesel saturation were similar to those of A2 and A3.

Table 1: Physical properties of peat columns in unsteady state immiscible transport experiments; *porosity of A1 is the average of A2 and A3

column	Porosity (%)	Hydraulic Conductivity (m/s)	Absolute Permeability (m^2)	Residual diesel saturation (S_{Nr})
A1	93%*	1.0×10^{-4}	1.0×10^{-11}	-
A2	93%	1.1×10^{-4}	1.1×10^{-11}	17%
A3	93%	5.6×10^{-5}	5.6×10^{-12}	17%
A4	90%	3.4×10^{-5}	3.3×10^{-12}	12%
B1	97%	3.5×10^{-4}	3.4×10^{-11}	4%
B2	97%	4.0×10^{-4}	3.9×10^{-11}	5%
B3	96%	6.4×10^{-4}	6.3×10^{-11}	7%

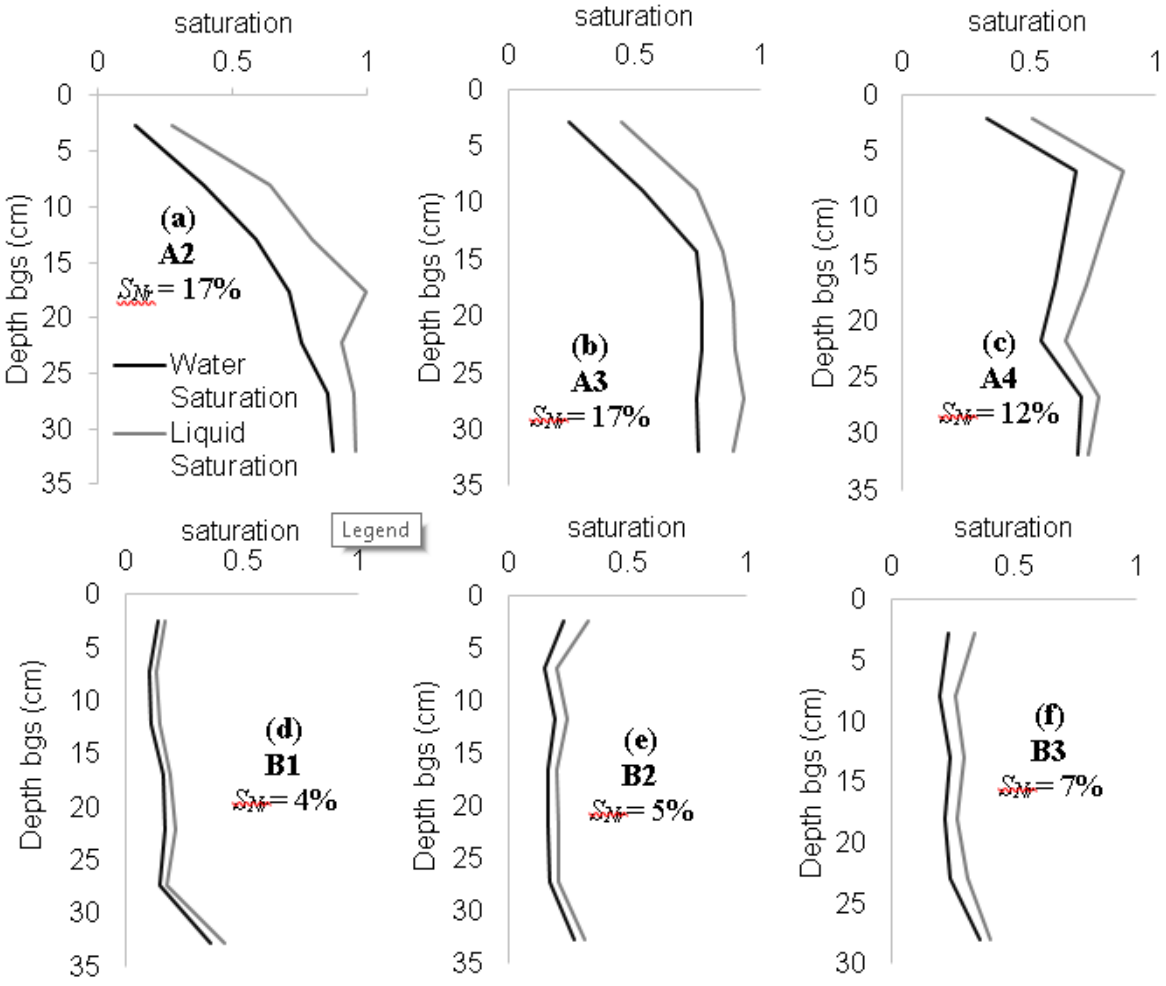

Figure 6: Variations of liquid saturation and water saturation with depth below ground surface (bgs) (top of each column) in the experimented columns of core A and core B;S_{Nr} is residual NAPL (diesel) saturation in the column.

3.1. Measured and estimated P_c-S-k_r relations

Each 1D immiscible displacement column test had a two-phase flow period, which started with diesel percolation into the pore space and ended when declining diesel head reached the peat surface, following which a three-phase flow period occurred as air imbibed into the peat column. The cumulative water and diesel production trends in the two-phase flow period of the immiscible displacement experiments were used in inverse modeling simulations. The boundaries imposed on

the unknown parameters in the inverse modelling simulations are presented in Table 2. Figure 7 illustrates the variations of measured and simulated cumulative production of water and diesel. The rate of diesel percolation into the pore space, which is the sum of the slopes (sum of first derivatives) of water and diesel cumulative production curves (in Figure 7), is larger in peat B than in peat A. The higher diesel percolation rate in peat B corresponded with the higher hydraulic conductivity in peat B columns.

Table 2: Ranges of uncertain/unknown parameters in random search simulations

	Brooks and Corey's Model (BCM)			**Power Law Model (PLM)**		
column	S_{wirr}	P_{cth} (Pa)	λ	S_{wirr}	n_w	n_N
A1	10-30%	20-100	0.1-7	45-55%	5-7	5-7
A2	10-70%	20-100	0.1-7	10-70%	2-7	2-7
A3	10-70%	20-100	0.1-7	10-70%	0.8-7	0.8-7
A4	60-75%	20-100	0.1-7	10-70%	0.8-7	0.8-7
B2	10-70%	20-100	0.1-7	25-50%	2-7	2-7
B3	10-70%	20-100	0.1-7	35-70%	2-7	2-7

The *RMSE* of all columns are less than 6.1 mL (Table 3). The error factor, expressed as the ratio of *RMSE* to the total produced diesel volume during the two-phase flow period (V_{diesel}), is less than 3.2% for BCM and less than 3.1% for PLM, showing that both BCM and PLM relations can accurately describe diesel percolation and outflow rates. Also, the water relative permeability curves obtained for a column by calibrating BCM (black lines in Figure 8), are in good agreement with the corresponding curve estimated using PLM (black dashed lines in Figure 8).

The estimated BCM parameters show that for intact peat cores the estimated irreducible water saturation (S_{wirr}) ranges between 29.9-47.5% for peat A and between 10.6%-26.0% for peat B. In PLM model estimations, S_{wirr} ranges between 46.7-55.8% for peat A and between 25.1-35.0% for peat B. Independent of the P_c-S-k_r model used, S_{wirr} in peat A is higher than that in peat B. The curvature of water relative permeability (n_w) using the PLM had a narrow range between replicates of peat A (5.07-5.83), and a narrow (but lower) range between replicates of peat B (2.01-2.52).

Table 3: estimated parameters of P_c-S-k_r relations

Brooks and Corey's Model (BCM)					
column	S_{wirr}	P_{cth}	λ	***RMSE* (mL)**	**Error (%) ($RMSE/V_{diesel}$)**
A1	29.9%	50.0	0.382	1.86	1.6%
A2	45.8%	29.9	0.705	3.28	2.4%
A3	47.5%	20.7	0.488	6.09	3.2%
A4	61.2%	30.4	3.39	0.84	0.5%
B2	10.6%	30.3	5.88	1.26	1.4%
B3	26.0%	21.1	7.00	1.76	1.1%
Power Law Model (PLM)					
column	S_{wirr}	n_w	n_N	***RMSE* (mL)**	**Error (%) ($RMSE/V_{diesel}$)**
A1	50.0%	5.83	5.46	3.71	3.1%
A2	46.7%	5.61	2.00	3.04	2.2%
A3	55.8%	5.07	2.00	5.83	3.1%
A4	61.8%	3.39	2.30	0.79	0.4%
B2	25.1%	2.01	2.82	1.39	1.5%
B3	35.0%	2.52	4.59	0.738	0.5%

Generally, in a given column, S_{wirr} obtained from BCM and PLM simulations (Table 3) are similar, thought they differ A1 and B2 columns. For example, for A2, S_{wirr} determined from BCM and PLM simulations are respectively 45.8% and 46.7% which are almost identical. However, in A1, the S_{wirr} values are 29.9% and 50.0% from BCM and PLM, respectively. The difference is likely due to the limitations of BCM, which is unable to describe water and NAPL relative permeability curves with low curvatures (note the generally poor fit between BCM derived NAPL relative permeability curves and data, in Figure 8). Details on the cause of differences are provided in Appendix D.

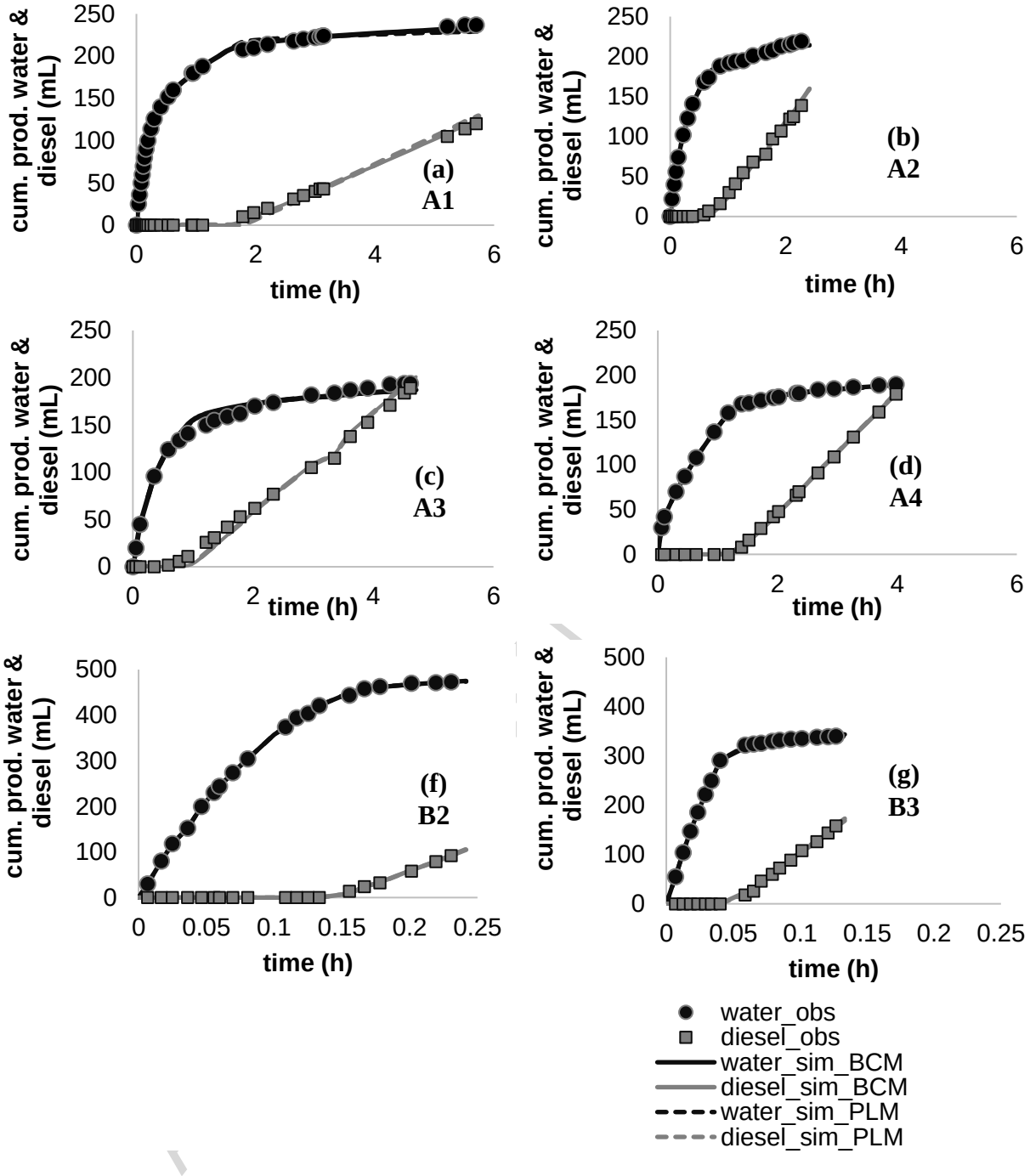

Figure 7: Measured and simulated cumulative production curves of water (black curves and circles) and diesel (grey curves and squares) during the two-phase flow period in the experimental peat columns; note the different scales in the x- and y-axes for the different peat types.

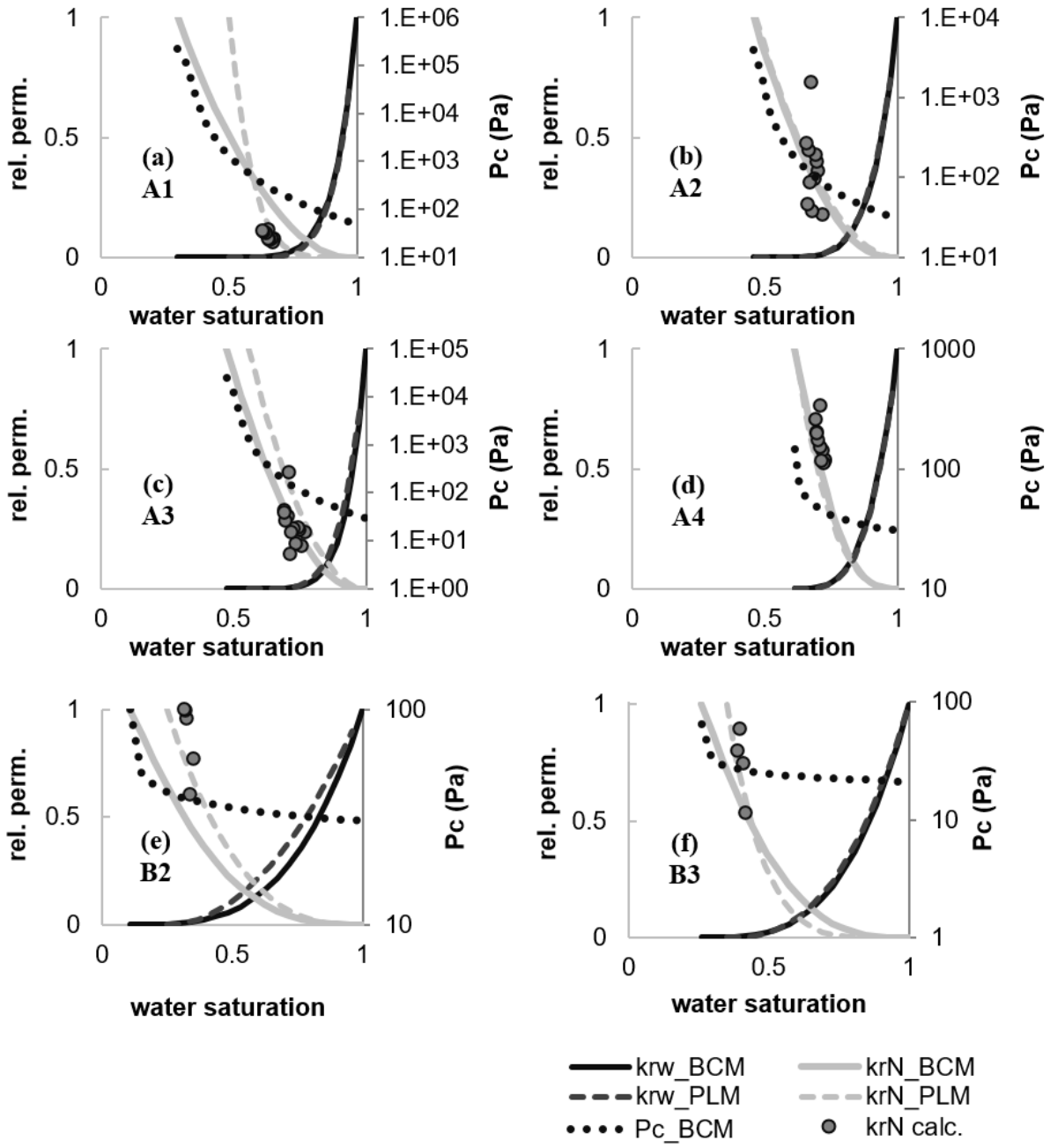

Figure 8: estimated water relative permeability (k_{rw}), diesel relative permeability (k_{rN}) and capillary pressure (Pc) curves using Brooks and Corey's model (BCM), and power-law model (PLM); grey circles illustrate diesel relative permeability measured using diesel outflow data.

3.2. Peat box

Twenty minutes after the spill started, traces of diesel were observed (visually) accumulating at the center of the peat box above the WT. Forty minutes after the spill began, diesel accumulation above the WT and across the chamber (not just in center) was observed. Approximately 4.7 hours after the spill began, the apparent diesel thickness above WT was ~6.5 cm uniformly distributed across the main chamber, and through the diesel migration to the left side well via the screens, 1.5 cm diesel was at the left well. Approximately 7.7 hours after the spill, the diesel thickness at the left side well was 5.7 cm, and the apparent thickness of diesel layer within peat was 5.8 cm. The rate of change of diesel layer thickness slowed down after this time. After 21.7 hours the thickness of the diesel layer in the left well and within the peat box both were 6.1 cm. Two days after spill, the thicknesses of diesel were 6.2 cm and 6.1 cm in the left well and in peat, respectively. One week after the spill the thicknesses were, respectively, 6.2 cm and 6.4 cm in the left well and in the peat box.

During this one-week period diesel did not flow into the right well due to a clogged screen, so the clogging was removed allowing redistribution of diesel to a similar thickness in both side wells and in the main chamber. After 8 days the diesel that had collected above the WT in the side wells was pumped out. This simulates lateral redistribution of diesel in a natural peatland, or pumping diesel in collection ditches excavated around a spill zone. Approximately 1525 mL of diesel were pumped out during the following two weeks period, representing ~82% of the 1858 mL of the spilled diesel, which had migrated laterally to the side wells after reaching the water table.

The first infiltration event, equivalent to ~5 cm of water over 1.3 hours, caused a WT rise of 6 cm. As the WT returned to its pre-rainfall level, 5 mL of diesel was released from the pore spaces to the side wells. The second rainfall was equivalent of 4.8 cm of water over 1.3 hours, causing a WT rise of 6.7 cm. No additional diesel flowed out as the WT returned to its pre-rainfall condition. At the end of experiment, dropping the WT to the bottom of the sample released 12 mL of diesel.

Figure 9 illustrates the spatial distributions of porosity, diesel saturation, and water saturation in the peat box at the end of the experiment. The porosity ranged from 92.4% to 98.0, and although

scattered horizontally within a layer, generally declined with increasing depth down the peat profile. On average the porosity in the right side of the chamber was less than in the center and left side of the monolith. Water retained by capillary forces was higher on the right side and with depth.

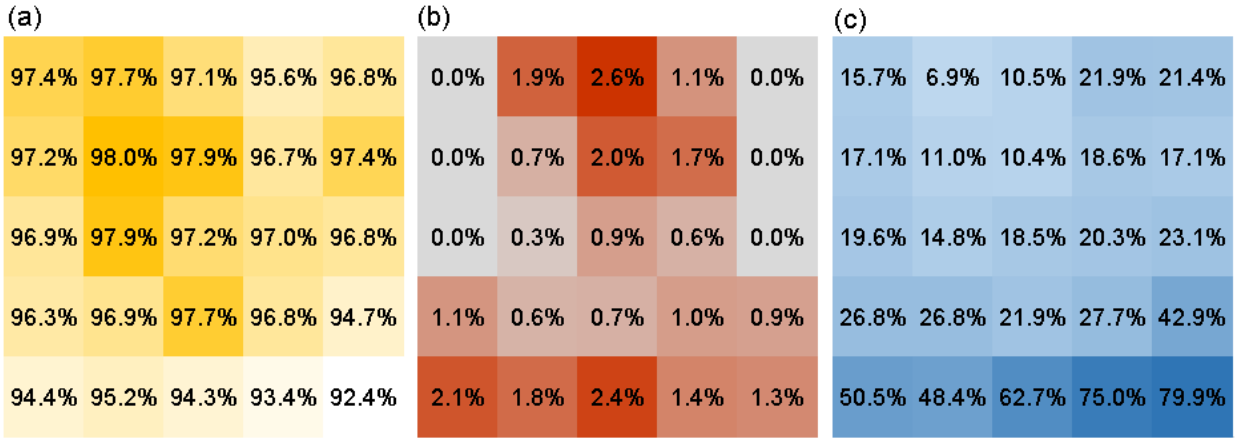

Figure 9: Spatial distribution of porosity in the peat box; value in each segment is (a) the porosity, (b) diesel saturation, and (c) water saturation of the segment; higher values in each figure are illustrated with more intense color.

The residual diesel saturation in the contaminated peat in the peat box experiment varied between 0.3% and 2.6%, with higher residual saturation in the central segments (0.7%-2.6%), reflecting the placement of the spill over the central 20 cm of the peat. No lateral dispersion of diesel into the side blocks at the top 30 cm of the peat occurred. The volume of diesel removed from the system due to lateral migration over the first 7 days, both simulated infiltration events, and final drainage was 1525, 5, and 12 mL, respectively. The volume of residual diesel in the drained monolith was 241 mL. Hence, of the 1860 mL spilled volume, 77 mL (~4% of initial spill volume) of diesel was unaccounted for, representing the mass balance error. The measured resistance values were inconsistent, experienced drift and a distinct diurnal oscillation and displayed no relation to diesel presence in pore space. Consequently, resistance values were considered spurious, and were rejected.

4. Discussion

Previous studies have quantified water contact angle on soils with different organic carbon content. Bradford and Leij (1995a, 1995b) and Ramírez-Flores et al. (2010) reported the contact angle of water in a water-air system on sand and silt as 0°. With respect to organic soils, Michel et al. (2001) reported water contact angles on moderately decomposed peat at different matric potentials ranged from 69.0° at a partially saturated condition (water potential of -32 kPa) to 106.4° at a dry condition (water potential -100 MPa). Although Michel et al. (2001) did not characterize water contact angle in the water potential of ~0 kPa (when air is imbibing into a saturated peat sample), the inverse relation of water contact angle with water potential in their study suggests that the contact angle at the saturated condition would be less than 69.0°, which compares to the value obtained here (51.7°). Regarding NAPL contact angle in NAPL-air systems, Ethington (1990) measured contact angle of benzene, toluene, and several other organic liquids on the surface of quartz and calcite, using the sessile drop method. Based on their study, contact angles of benzene and toluene on quartz in the presence of air was 11°-12° and 9°, respectively. The contact angles of NAPLs in the presence of air and on organic surfaces (61.2°) have not been reported elsewhere in literature.

Scaling measured diesel-air P_c-S data to the water-air system successfully matched measured water-air P_c-S relations. This suggests water retention data available for different types of Canadian peat soils could be scaled to other fluid-fluid systems using representative interfacial tensions and contact angles. In the case of a diesel spill onto a peatland, diesel-water and diesel-air capillary pressure data might be estimated using corresponding contact angles and the available water retention curves of the contaminated peat. In this study, diesel-air and water-air contact angles on peat were measured as 51.7° and 61.2° for the liquid drainage conditions. Gharedaghloo and Price (2017) have reported water contact angles on peat in the presence of diesel during water drainage and water imbibition. If a hydrocarbon liquid other than diesel is spilled on a peatland, similar methodology could be applied to determine corresponding contact angles and to scale the capillary pressure data using appropriate interfacial tensions.

The saturated hydraulic conductivity of peat A and peat B in the 1D column test were in agreement with the literature. McCarter and Price (2014) reported the hydraulic conductivity of peat A ranging between 6.9×10^{-5} m/s to 5.2×10^{-4} m/s between surface and 27.5 cm below ground surface (bgs). The harmonic mean of the values reported in their study is ~ 1.9×10^{-4} m/s which is similar to the values of this study in the 1D columns of peat A (Table 1). In the regards of peat B, Price et al. (2008) reported the variation of saturated hydraulic conductivity of the peat B ranging from 1.8×10^{-3} m/s at 5cm bgs to 2.4×10^{-4} m/s at 25 cm bgs with a harmonic mean of 3.3×10^{-4} m/s; as a comparison, the saturated hydraulic conductivity of peat B ranged from 3.5×10^{-4} m/s to 6.4×10^{-4} m/s (Table 1) which are similar to harmonic mean from value from Price et al. (2008).

In columns A1 and A4 the global minimum for a wide range of parameters uncertainty did not match the calculated diesel k_r data. Therefore, the upper and lower bounds of the uncertainty ranges of the parameters were limited to ensure k_r-S curve of diesel (grey lines in Figure 8) were close to the measured points (grey circles in Figure 8). The agreement between the measured points and the k_r-S curves of diesel (Figure 8) and the acceptable match between measured and simulated production curves of water and diesel (Figure 7), which is reflected in low *RMSE* and error factors (Table 3), show that the Brooks and Corey's (1964) model (Equation 4 to Equation 7) and the power law model (Equation 8 and Equation 9) can be used to model diesel flow and production in the column tests. We note, however, that the result of PLM had less inconsistency with the measurements, showing the relative accuracy of this model compared to BCM. While there are other relative permeability models (e.g. Chierici 1984; Huang et al. 1997), they have more parameters, which increases the risk of uncertainty and non-uniqueness in model parameterization.

In addition to the mentioned models, the P_c-S-k_r model of Van Genuchten (1980) (VG), which has been shown to efficiently describe the flow and retention of water in the presence of air in unsaturated peat (e.g., Schwärzel et al. 2006; Price et al. 2008), was also excluded from the inverse modeling simulations. It is well known that the water k_r-S relation in peat is a convex curve (e.g., Price et al. 2008; McCarter et al. 2014), and a convex curve of water k_r-S in VG model is associated with concave trend of NAPL k_r-S (e.g., Fig 5 of Luckner et al. 1989). This means using the VG model results in a concave curve for the NAPL k_r-S relation in the inverse modelling calculations. However, the directly calculated NAPL relative permeability data (grey circles in Figure 8)

demonstrates that k_r-S relations of NAPL in the experimented peats have convex trends (in linear axes), which causes VG to be not useful in this particular study and be excluded from inverse modelling simulations.

Peat columns comprising peat from the same source had similar water relative permeability curves (Figure 10). The water relative permeability curves of peat A (black curves) and peat B (grey curves) form separate clusters illustrating their distinct water relative permeability trends. This similarity was reflected in similarity of relative permeability model parameters; for example the estimated n_w parameter of PLM ranged between 5.07-5.83 in A1-A3 columns of peat A and between 2.01-2.52 in columns of peat B (Table 3). In another example, the irreducible water saturation (S_{wirr}) of PLM ranged between 46.7-55.8% in A1-A3 columns of peat A and between 25.1-35.0% in B2-B3 columns of peat B showing similarities within a type of peat and differences between two different peat types. The results showed that both S_{wirr} and n_w increased with bulk density of peat. Price at al. (2008) presented unsaturated hydraulic conductivity (K_{unsat}) of water in peat B (i.e., extracted from the same site) taken between 0-25 cm below ground surface (bgs). The calculated k_{rw} data from their study (grey circles in Figure 10) reasonably compare with k_{rw} of peat B obtained in our study (grey lines in Figure 10). This suggests that in the absence of water relative permeability data for NAPL imbibition conditions, the unsaturated hydraulic conductivity of peat could be used to determine a reasonable estimate of the k_{rw}-S relation.

At a given water saturation, peat B has higher k_{rw} compared to peat A (Figure 8, Figure 10). The physical properties of the tested columns (Table 1) shows that peat A was more compacted and had smaller pore sizes compared to peat B. The amount of diesel saturation that reduces water relative permeability to $k_{rw} \leq 0.01$ is ~30% in peat A, while it is ~60-70% in peat B. This is likely due to a higher frequency of macro-pores and active pores in peat B compared to peat A, so that during diesel imbibition, a given saturation of diesel occupies a smaller fraction of active porosity of peat B compared to that of peat A. Consequently water flow is diminished less in peat B and the degree of k_{rw} reduction with increasing NAPL saturation is greater in peat A (Figure 10). Irreducible water saturation (S_{wirr}) of peat A (46.7-61.8%) was higher than that of peat B (25.1-35.0%) (Table 3). This is similar to the variations of residual water content in water-air system where reduction of peat hydraulic conductivity, which takes place typically down the peat profile

due to peat compaction and decomposition, is associated with increasing residual water content (Price and Whittington 2010; Goetz and Price 2015).

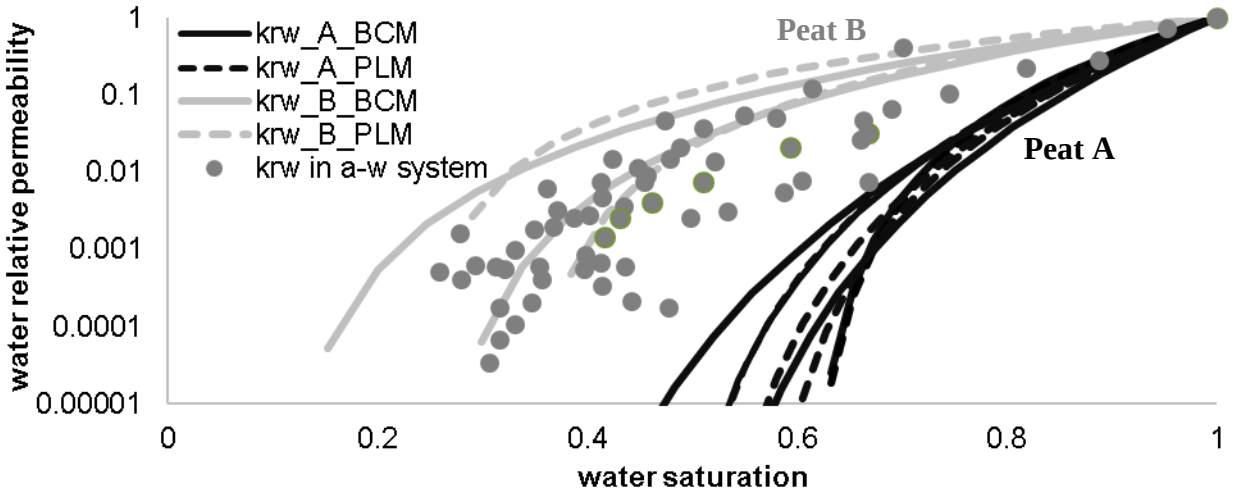

Figure 10: Estimated relative permeability curves from two-phase diesel-water flow (curves) for core A (black curves) (A1, A2, and A3 columns) and core B (grey curves) (B2 and B3 columns), and measured water relative permeability in water-air system (grey circles) from Price et al. (2008), taken from the same peatland.

The A1 to A3 and B1 to B3 columns in the 1D column tests were cut out of undisturbed peat blocks; the similarities in the results of replicates within each peat type suggests that if peat is sampled with care to preserve its pore structure, a consistent parameter set can be derived, at least for a local scale. The similarity between the relative permeability relations and residual diesel saturation between intact columns of peat A (A1, A2, A3) and the compacted column (A4), may be due to their similar porosity and hydraulic conductivity. This suggests using disturbed peat samples might be more representative than using intact peat from a different peatland with different porosity and permeability.

In one dimensional immiscible displacement column tests, the residual saturation was higher in peat A compared to that in less dense peat B (Figure 6). Furthermore, the diesel percolation rate varied between peat types and was proportional to hydraulic conductivity. This, in association with the increase of residual diesel saturation with peat density, leads to faster percolation and higher risk of lateral diesel migration in peatlands with less dense peat. The results also suggest that, due

to variation of peat density and hydraulic conductivity between hummocks and hollows (Baird et al, 2016), diesel percolation rate and the residual diesel saturation could vary substantially within a peatland. Due to shallower water table depth in hollows compared to hummocks, diesel percolation to the water table will likely happen earlier in hollows. This might lead to continuous NAPL phases and NAPL movement in the connected hollows, which is similar to that found for dissolved contaminants in the connected hollows of a bog peatland (Balliston 2017).

In the 1D column experiments, before air imbibition, macro-pores of the peat columns were drained and diesel replaced water in those pores. However, in the peat box experiment and during the spill, due to the rapid infiltration of diesel and limited rate of diesel spill, the vadose zone of the peat stayed unsaturated containing all three phases of water, diesel and air. Consequently, the maximum diesel saturations in 1D columns were higher than that in the vadose zone of the peat box. The residual NAPL saturation is positively correlated with maximum NAPL saturation before air imbibition (Van Geel and Roy 2002), which means higher residual saturation of diesel in the column experiments. This explains why the residual diesel saturation in peat B in the column experiments (4-7%) was higher than that in the same peat in the peat box experiment (0.3-2.6%.).

In the 2-D experiment, nearly 77 mL of diesel was unaccounted for based on the mass balance calculations. The mass balance error could be due to retention of liquid hydrocarbons in the peat matrix even after air-drying and volatilization (Jarsjö et al. 1994). Furthermore, some methodological error associated with estimating the residual volume could have contributed to the difference. The predictability of the compression technique and estimation of the residual diesel volume has been demonstrated (Appendix A and Figure A.1); the error associated with this method is insignificant (Appendix B and Table B.1). Nevertheless, the error of estimation might be proportionately high with very low volumes of NAPL, because NAPL's constituents can be absorbed to the organic matter in peat matrix (Jarsjö et al. 1994), thus not become remobilized via compression.

At diesel saturation of 1-S_{wirr}, diesel relative permeability tends to 1, meaning that diesel effective permeability becomes equal to the absolute permeability of the peat column. Due to the large capillary pressure threshold of micro-pores, diesel does not percolate into the dead-end pores and the inactive porosity of peat (Gharedaghloo and Price, 2017), occupying only active porosity

including macro-pores. Thus, if the diesel effective permeability equals the absolute permeability, 1-S_{wirr} is the portion of the porosity in which fluid flow takes places. This means 1-S_{wirr} corresponds to the active porosity, suggesting that the flooding of saturated peat with diesel might be a dynamic and flow-based method for characterizing active and inactive porosities of peat; so far the active porosity has been characterized with static and non-flow based methods (e.g. Hoag and Price 1997; Quinton et al. 2009; McCarter and Price, 2017; Rezanezhad et al. 2009, 2012).

In cases where spilled liquid is compositionally similar to diesel, the sum of water-NAPL (σ_{wN}) interfacial tension (28.9 mN/m for diesel-water; Environment Canada 2018) and NAPL-air (σ_{Na}) interfacial tension (23.8 mN/m for diesel-air; Environment Canada 2018) is less than water-air (σ_{wa}) interfacial tension (i.e. $\sigma_{wa}>\sigma_{wN}+\sigma_{Na}$). Physically this means a thin film of NAPL remains between the air and water phases in the contaminated pores, minimizing the surface energy of the system. Based on Chatzis et al. (1988) and Kantzas et al. (1988) the NAPL film spreading between water and air enhances NAPL drainage and reduces its retention. Sohrabi et al. (2000) demonstrated that in such condition an iterative imbibition of the water phase and a gas phase (e.g. air) could reduce the NAPL retention and enhance its recovery from pore space. In a contaminated peatland, the iterative imbibition of water and air could take place due to frequent rainfall events and the consequent water and air invasions to the NAPL contaminated zone. In the peat box experiment, 5 mL of diesel were released after the first rainfall and during the WT drawdown, which could be due to the iterative water and gas invasion. In a field condition the iterative invasion of water and air could potentially remobilize residual NAPL from the contaminated zone. This suggests that manipulated fluctuations of the water table might be an appropriate strategy for reducing residual NAPL in the spill zone of a contaminated peatland.

5. Conclusion

For the first time, relative permeability of a NAPL in peat pore space was estimated and P_c-S-k_r model parameters were characterized. The relative permeability of water determined through inverse modelling was in good agreement with measured data of Price et al. (2008); this suggests

that if the relative permeability relations of water in peat in the two-phase NAPL-water system are not available, measured unsaturated hydraulic conductivity data could be a close estimate of them.. The relative permeability relations of diesel obtained via inverse modelling were in good agreement with those relations that were obtained via direct calculations (Figure 8). The water and NAPL relative permeability relations are needed by environmental scientists and groundwater modellers in predicting the NAPL migration in contaminated peatlands after a NAPL spill accident. However, it must be noted that to be able to make a reasonable numerical prediction of the behavior of NAPL in a peatland, a larger number of samples, accounting for spatial variability including from different layers of peat, are required. Having a larger sample of experimental results would lead to more representative P_c-S-k_r relations for the contaminated peat, which is essential when trying to upscale numerical simulations with cells or elements larger than the scale of laboratory experiments.

The diesel percolation rate and its retardation in the vadose zone of the peat layer was shown to be a function of peat pore structure. The percolation rate increased in peat with lower bulk density, while residual diesel saturation increased with bulk density. The residual diesel saturation in peat varied between 0.3-17% depending on the spill scenario and physical properties of the peat. The variation of residual diesel saturation with water table depth in a given peat implies that the residual diesel saturation depends on moisture regime and thus potentially on the time of year in which the spill occurs. In the case of a hydrocarbon spill onto a peatland, these results could be used to determine if the downward percolating free-phase NAPL will be retained by peat in the vadose zone, or if the volume of free-phase hydrocarbon is large enough to pass the vadose zone and arrive at the water table.

In the peat box experiment and when water table was ~40 cm below ground surface, more than 80% of the spilled diesel reached water table and migrated laterally to the side wells. In a shallower water table condition, the total volume of residual diesel left in the narrower vadose zone would be less compared to deep water table conditions, so the fraction of spilled diesel migrating to the side wells would be greater. In a natural peatland setting, excavating ditches at the down-gradient face of the free-phase plume's edge might be an efficient option for recovering spilled LNAPL. If the volume of spilled NAPL is large enough for it to pass through the vadose zone and reach the

water table, the ditches could collect the mobile portion of the spilled NAPL. The results also suggest that water table fluctuations could remobilize NAPL present in peat vadose zone meaning that artificially fluctuating the water table in the source zone could reduce the residual NAPL in the vadose zone.

Acknowledgements

We would like to thank Wetlands Hydrology Research Laboratory, especially James Sherwood and Celeste Cameron for assistance in the lab. The research was funded by a NSERC Discovery Grant (174626-2013-RGPIN) to Dr. Price.

Appendix A: Estimating diesel and water volumes in contaminated peat

A traditional method of obtaining residual NAPL saturation (S_{Nr}) is retort distillation in which the NAPL-containing soil (or rock) sample is placed in a chamber, and the temperature is raised above 500°C to evaporate water and NAPL from the sample. Then, the released vapors are condensed giving the original water and NAPL mass in the soil sample (API, 1998). However, this method cannot be employed for peat soils since at the temperatures of ~ 500°C the contaminated peat would burn away. A potential alternative method would be to place the NAPL contaminated sample in a Dean-Stark apparatus from which the water is removed by distillation and the NAPL is extracted with a solvent (e.g. toluene) (API, 1998). However, this method would dissolve the natural hydrocarbons and waxes present in the peat matrix and cause errors.

A method that was sufficiently simple and could be repeated for heavy masses of NAPL-containing peat and a large number of peat samples was in need. A cylindrical apparatus with an outflow was constructed in which by using a hydraulic press contaminated peat samples are compacted and the liquids present in peat pore space are released and collected from the outflow valve. To determine diesel and water volumes remaining in peat pore space, peat was squeezed

with the hydraulic press up to pressure of ~120 atm. Compacting peat removed in average 73% of pore fluids in each column test; the rest of the liquids remained in the compacted peat, which could cause error in the estimations. To overcome this issue, it was assumed that the volumetric ratio of liquids that were squeezed out of the contaminated peat sample during the pressing was the same as the ratio of their in-situ saturations. Using the primary weight of the peat (containing water and diesel), the dry weight of peat after drying the compacted peat for 7 days, and the volumetric ratios of liquids in the sample (from the pressing), in-situ volumes and saturations of water and diesel were estimated for the contaminated peat sample.

To test the accuracy of this method, 20 grams of milled peat were mixed with known volumes of diesel and water at varying ratios. The mixtures were then pressed, and then using the approach noted above the volumes of diesel and water in the mixture were estimated. Figure A. 1 compares the actual and estimated volumes of liquids in the evaluation tests showing that the estimating method does not overestimate or underestimate the water and diesel volumes in peat samples, and the error associated with estimations is negligible. It should be noted that this method is specific to peat soils and for the conditions that NAPL saturation is high enough and NAPL can mobilize and flow out of the pore space by pressing. The advantage of this method is its simplicity and its potential for use in the field. The disadvantage is that it might perform poorly at low and non-mobile ranges of NAPL concentrations.

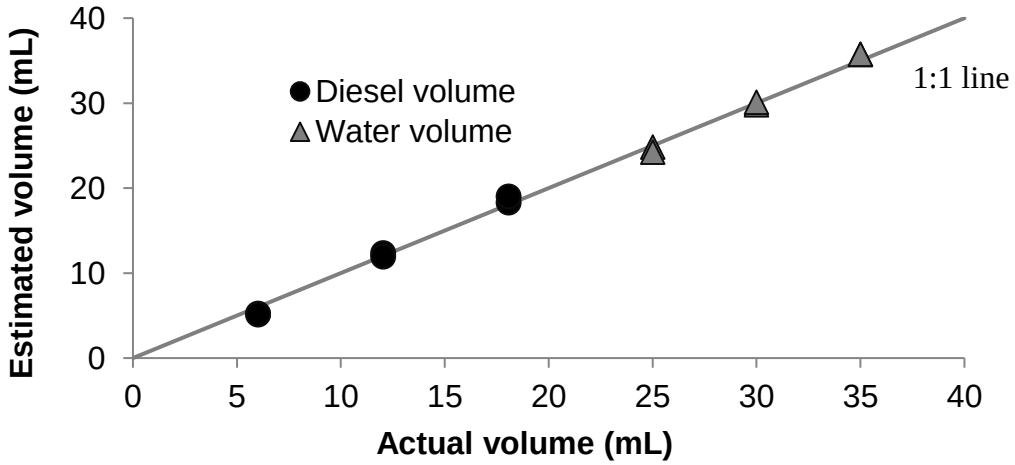

Figure A. 1: Actual and estimated volumes of water and diesel in peat pressing tests

Appendix B: mass balance in one dimensional peat column experiments

Using the assumption discussed in Appendix A, peat segments from column tests were pressed and the extracted volumes of each phase and the total liquid weight of each segment were used to estimate in-situ volumes of water and diesel along each column. Table B.1 shows the error in diesel mass balance is under 5 mL (up to 1.3% of spilled diesel volume). This means the estimated volumes of diesel inside columns are similar to actual values and the estimations did not introduce large errors in estimated diesel volumes of each column.

Table B.1: summary of mass balance of diesel in the peat column experiments; where $V_{spilled}$ is volume of diesel initially placed above the water saturated peat column, $V_{outflow}$ is volume of diesel that flowed out of the column bottom by the end of the experiment, V_{column} is the estimated volume of diesel remaining inside the column; $Error_{volume}$ is the volumetric error of diesel mass that is missing due to assumptions, and *Error* is the percentage of missing to total volume.

Column	$V_{spilled}$ (mL)	$V_{outflow}$ (mL)	V_{column} (mL)	$Error_{volume}$ (mL) ($V_{spilled}$-$V_{outflow}$-V_{column})	*Error* ($Error_{volume}/V_{spilled}$)×100%
A2	367	256	112	-1	-0.3%
A3	395	283	107	5	+1.3%
A4	368	297	75	-4	-0.9%
B1	356	329	26	1	+0.3%
B2	578	536	37	5	+0.9%
B3	513	475	40	2	+0.4%

Appendix C. Preparing pressure transducers

Hydrophobic porous ceramic are required to measure NAPL pressures in the system. Several studies have chemically treated porous ceramics to change their wetting tendency and to obtain hydrophobic ceramics facilitating measurement of NAPL pressure with transducers. Lenhard and Parker (1988) used chlorotrimethysila and Ahmed and Van Geel (2009) used octadecyltrichlorosilane as the chemicals for treating the porous ceramics. A similar chemical, Dichlorodimethylsilane (Sigma-Aldrich) was used in this study. Clean dry porous ceramic cups (Soilmoisture Equipment Corp, USA) were placed in 50:50 (vol/vol) mixture of

Dichlorodimethylsilane and benzene (EMD Millipore, GR grade, purity>99%) for 1 week. The bottle containing mixture and the porous cups was shaken once every 24 hours to promote the chemical reaction between Dichlorodimethylsilane and ceramic cups. After 1 week the ceramics were dried in the fume hood for 24 hours, and then were placed in kerosene for 24 hours to remove residual free Dichlorodimethylsilane from the ceramic cups (suggested by Ahmed and Van Geel 2009). Then, the treated ceramic cups were used in assembling the NAPL pressure transducers. Untreated porous ceramic cups were used in assembling water pressure transducers. The NAPL and water transducers were filled respectively with diesel and water; the filling process and air removal process was done iteratively to leave no air bubbles in the main chambers of the transducers. Finally, the transducers were inserted into the peat body in a way that each porous cup was 5 cm within the peat body. Out of 8 NAPL (diesel) and 8 water pressure transducers, 6 NAPL and 6 water pressure transducers were above the initial water table, and two of each type were below the initial water table.

Appendix D: Causes of the differences in the estimated S_{wirr} between BCM and PLM models

For λ ranging between 0.1-7 the power of k_{rw} curve varies in 3.3-23; therefore, if the power of k_{rw} relation of the media is less than 3.3 (i.e. the k_{rw} curve has low curvature), the BCM model will fail to describe the k_r-S relation of water in the medium. In this case, the optimization function that is minimizing the error between observed and simulated production curves cannot match the production curves by adjusting λ, and instead, will adjust S_{wirr} (to less realistic values) to produce required k_{rw} values in mid ranges of water saturations. On the other hand, PLM does not contain the curvature limitation and can describe and produce low curvature k_r-S relations with power less than 3.3. In addition, water and NAPL relative permeability relations in BCM are correlated by λ. Based on the equation of k_{rN} in BCM (Equation 7), the curvature of k_{rN} relation has a higher and a lower limit, which can add to the risk of unrealistic S_{wirr} in the BCM model in the optimization process. The ability of the PLM model in producing k_r-S curvatures that are out of the bounds of BCM could explain why the RMSE from PLM simulations is generally less that of BCM results

(Table 3). The inability of BCM model in producing low curvatures in relative permeability curves and the co-dependence of water and NAPL k_r-S relations in this model could be the reasons that S_{wirr} determined from BCM is less than that from the PLM. It must be noted that irrespective of the difference between values of S_{wirr} in these models, the k_r-S curves obtained from PLM and BCM simulations, especially those of water, are very similar graphically (Figure 8). In summary, BCM limitations in producing low curvatures in the relative permeability relation may render it less accurate than PLM.

References

Ahmed, M. E., & Van Geel, P. J. (2009). Potential concerns related to using octadecyltrichlorosilane (OTS) in rendering soils and porous ceramics hydrophobic. *Journal of contaminant hydrology*, *110*(1-2), 22-33.

API, Recommended Practices for Core Analysis, 2nd Edition, February 1998.

Baird, A. J., Milner, A. M., Blundell, A., Swindles, G. T., & Morris, P. J. (2016). Microform-scale variations in peatland permeability and their ecohydrological implications. *Journal of Ecology*, *104*(2), 531–544. http://doi.org/10.1111/1365-2745.12530.

Balliston, N. (2017). Saturated and vadose zone fate and transport of a continuously released tracer in a sub-arctic bog peatland. Masters thesis, University of Waterloo, UWSpace. http://hdl.handle.net/10012/11333.

Bradford, S. A., & Leij, F. J. (1995a). Wettability effects on scaling two-and three-fluid capillary pressure-saturation relations. *Environmental science & technology*, *29*(6), 1446-1455.doi:10.1021/es00006a004.

Bradford, S. A., & Leij, F. J. (1995). Fractional wettability effects on two-and three-fluid capillary pressure-saturation relations. *Journal of Contaminant Hydrology*, *20*(1-2), 89-109. doi:10.1016/0169-7722(95)00027-s.

Brooks, R., & Corey, T. (1964). Hydraulic Properties of Porous Media. *Hydrology Papers, Colorado State University*, *24*.

Caudle, B. H., Slobod, R. L. and Brownscombe, E. R. (1951). Further developments in the laboratory determination of relative permeability. *Journal of Petroleum Technology*, 3(05), 145-150. doi:10.2118/951145-g.

Chardaire-Riviere, C., Chavent, G., Jaffre, J., Liu, J. and Bourbiaux, B. J. (1992). Simultaneous Estimation of Relative Permeabilities and Capillary Pressure. *Society of Petroleum Engineers Formation Evaluation*, 7(04), 283–289. doi:10.2118/19680-pa.

Chatzis, I., Kantzas, A., & Dullien, F. A. L. (1988). On the investigation of gravity-assisted inert gas injection using micromodels, long Berea sandstone cores, and computer-assisted tomography. In *Society of Petroleum Engineers Annual Technical Conference and Exhibition*. doi:10.2118/18284-ms.

Chierici, G. L. (1984). Novel relations for drainage and imbibition relative permeabilities. *Society of Petroleum Engineers Journal*, *24*(03), 275-276. doi: 10.2118/10165-pa.

Conrad, S. H., Glass, R. J., & Peplinski, W. J. (2002). Bench-scale visualization of DNAPL remediation processes in analog heterogeneous aquifers: surfactant floods and in situ oxidation using permanganate. *Journal of Contaminant Hydrology*, *58*(1-2), 13-49. doi:10.1016/s0169-7722(02)00024-4.

Crescimanno, G. and Iovino, M. (1995). Parameter estimation by inverse method based on one-step and multi-step outflow experiments. *Geoderma*, 68(4), 257-277. doi:10.1016/0016-7061(95)00049-8.

Darnault, C. J., Throop, J. A., DiCarlo, D. A., Rimmer, A., Steenhuis, T. S., & Parlange, J. Y. (1998). Visualization by light transmission of oil and water contents in transient two-phase flow fields. *Journal of Contaminant Hydrology*, *31*(3-4), 337-348.

Deiss, J., Byers, C., Clover, D., D'Amore, D., Love, A., Menzies, M. A., ... & Walter, M. T. (2004). Transport of lead and diesel fuel through a peat soil near Juneau, AK: a pilot study. *Journal of contaminant hydrology*, *74*(1-4), 1-18. doi:10.1016/j.jconhyd.2004.02.003.

Demond, A. H., & Roberts, P. V. (1991). Effect of interfacial forces on two-phase capillary pressure—saturation relationships. *Water Resources Research*, *27*(3), 423-437.doi:10.1029/90wr02408

DiCarlo, D. A., A. Sahni, and M. J. Blunt (2000), Three-Phase Relative Permeability of Water-Wet, Oil-Wet and Mixed-Wet Sandpacks. *Society of Petroleum Engineers Journal*, 5(01), pp.82–91. Available at: doi:10.2118/60767-pa.

Environment Canada, www.etc-cte.ec.gc.ca/databases/oilproperties/pdf/web_diesel_fuel_oil_(canada).pdf, retrieved: 18th June 2018.

Eching, S. O., & Hopmans, J. W. (1993). Optimization of hydraulic functions from transient outflow and soil water pressure data. *Soil Science Society of America Journal*, *57*(5), 1167-1175. doi:10.2136/sssaj1993.03615995005700050001x.

Ethington, E. F. (1990). *Interfacial contact angle measurements of water, mercury, and 20 organic liquids on quartz, calcite, biotite, and Ca-montmorillonite substrates* (No. 90-409). US Geological Survey.

Fagerlund, F., Illangasekare, T. H., & Niemi, A. (2007). Nonaqueous-phase liquid infiltration and immobilization in heterogeneous media: 1. Experimental methods and two-layered reference case. *Vadose Zone Journal*, *6*(3), 471-482. doi:10.2136/vzj2006.0171.

Gharedaghloo, B., & Price, J. (2017). Fate and Transport of free-phase and dissolved-phase hydrocarbons in peat and peatlands: Developing a conceptual model. *Environmental Reviews*.doi:10.1139/er-2017-0002.

Goetz, J. D., & Price, J. S. (2015). Role of morphological structure and layering of Sphagnum and Tomenthypnum mosses on moss productivity and evaporation rates. *Canadian Journal of Soil Science*, *95*(2), 109-124. doi:10.4141/cjss-2014-092.

Goldstein, L., Prasher, S. O., & Ghoshal, S. (2007). Three-dimensional visualization and quantification of non-aqueous phase liquid volumes in natural porous media using a medical X-ray Computed Tomography scanner. *Journal of Contaminant Hydrology*, *93*(1-4), 96-110. doi:10.1016/j.jconhyd.2007.01.013.

Hoag, R. S., & Price, J. S. (1997). The effects of matrix diffusion on solute transport and retardation in undisturbed peat in laboratory columns. *Journal of Contaminant Hydrology*, *28*(3), 193-205. doi:10.1016/s0169-7722(96)00085-x.

Høst-Madsen, J. and Jensen, K. H. (1992). Laboratory and numerical investigations of immiscible multiphase flow in soil. *Journal of hydrology*, 135(1-4), 13-52. doi:10.1016/0022-1694(92)90079-b.

Huang, D. D., Honarpour, M. M., & Al-Hussainy, R. (1997, September). An improved model for relative permeability and capillary pressure incorporating wettability. In *SCA* (Vol. 9718, pp. 7-10).

Illangasekare, T. H., Armbruster III, E. J. and Yates, D. N. (1995). Non-aqueous-phase fluids in heterogeneous aquifers—experimental study. *Journal of Environmental Engineering*, 121(8), 571-579. doi:10.1061/(asce)0733-9372(1995)121:8(571).

Jarsjö, J., Destouni, G., & Yaron, B. (1994). Retention and volatilisation of kerosene: Laboratory experiments on glacial and post-glacial soils. *Journal of contaminant hydrology*, *17*(2), 167-185. 167–185. doi:10.1016/0169-7722(94)90020-5.

Johnson, E. F., Bossler, D. P. & Bossler, V. O. (1959). Calculation of relative permeability from displacement experiments. *Society of Petroleum Engineers.*

Kantzas, A., Chatzis, I. and Dullien, F. A. L. (1988). Enhanced Oil Recovery by Inert Gas Injection. *Society of Petroleum Engineers Enhanced Oil Recovery Symposium*. doi:10.2118/17379-ms.

Kelly-Hooper, F., Farwell, A. J., Pike, G., Kennedy, J., Wang, Z., Grunsky, E. C., & Dixon, D. G. (2013). Is it clean or contaminated soil? Using petrogenic versus biogenic GC-FID chromatogram patterns to mathematically resolve false petroleum hydrocarbon detections in clean organic soils: A crude oil–spiked peat microcosm experiment. *Environmental toxicology and chemistry*, *32*(10), 2197-2206. doi:10.1002/etc.2285.

Kool, J. B., Parker, J. C., & Van Genuchten, M. T. (1985). Determining Soil Hydraulic Properties from One-step Outflow Experiments by Parameter Estimation: I. Theory and Numerical Studies 1. *Soil Science Society of America Journal*, *49*(6), 1348-1354. doi:10.2136/sssaj1985.03615995004900060004x.

Lenhard, R. J. and Parker, J. C. (1988). Experimental validation of the theory of extending two-phase saturation-pressure relations to three-fluid phase systems for monotonic drainage paths. *Water Resources Research*, 24(3), 373-380. doi:10.1029/wr024i003p00373.

Lenhard, R. J., Dane, J. H., Parker, J. C., & Kaluarachchi, J. J. (1988). Measurement and simulation of one-dimensional transient three-phase flow for monotonic liquid drainage. *Water Resources Research, 24*(6), 853-863. doi:10.1029/wr024i006p00853.

Leverett, M. C. (1939). Flow of oil-water mixtures through unconsolidated sands. *Transactions of the AIME, 132*(01), 149-171. doi:10.2118/939149-g.

Leverett, M., & Lewis, W. B. (1941). Steady flow of gas-oil-water mixtures through unconsolidated sands. *Transactions of the AIME, 142*(01), 107-116. doi:10.2118/941107-g.

Lide, D. R. (2012). CRC handbook of chemistry and physics.

Lie, K. A. (2016). An Introduction to Reservoir Simulation Using MATLAB: User guide for the Matlab Reservoir Simulation Toolbox (MRST). SINTEF ICT.

Luckner, L., Van Genuchten, M. T., & Nielsen, D. R. (1989). A consistent set of parametric models for the two-phase flow of immiscible fluids in the subsurface. *Water Resources Research, 25*(10), 2187-2193.

McCarter, C. P., & Price, J. S. (2014). Ecohydrology of Sphagnum moss hummocks: mechanisms of capitula water supply and simulated effects of evaporation. *Ecohydrology, 7*(1), 33-44. doi:10.1002/eco.1313.

McCarter, C. P., & Price, J. S. (2017). The transport dynamics of chloride and sodium in a ladder fen during a continuous wastewater polishing experiment. *Journal of Hydrology, 549*, 558-570. doi:10.1016/j.jhydrol.2017.04.033.

Michel, J. C., Rivière, L. M., & Bellon-Fontaine, M. N. (2001). Measurement of the wettability of organic materials in relation to water content by the capillary rise method. *European journal of soil science, 52*(3), 459-467. doi:10.1046/j.1365-2389.2001.00392.x.

Morgan, W. B., & Pirson, S. J. (1964, January). The effect of fractional wettability on the Archie saturation exponent. In *Society of Petrophysicists and Well-Log Analysts 5th Annual Logging Symposium*.

MRST: The MATLAB Reservoir Simulation Toolbox. www.sintef.no/MRST (2017a).

Mungan, N., & Moore, E. J. (1968). Certain wettability effects on electrical resistivity in porous media. *Journal of Canadian Petroleum Technology, 7*(01), 20-25. doi:10.2118/68-01-04.

O'Carroll, D. M., Phelan, T. J. and Abriola, L. M. (2005). Exploring dynamic effects in capillary pressure in multistep outflow experiments. *Water Resources Research*, 41(11). doi:10.1029/2005wr004010.

Oostrom, M., Hofstee, C. and Wietsma, T. W. (2006). Behavior of a viscous LNAPL under variable water table conditions. *Soil & Sediment Contamination*, 15(6), 543-564. doi:10.1080/15320380600958976.

Palomino, A. M. and Grubb, D. G. (2004). Recovery of dodecane, octane and toluene spills in sandpacks using ethanol. *Journal of Hazardous Materials*, 110(1-3), 39-51. doi:10.1016/j.jhazmat.2004.02.035.

Pantazidou, M., & Sitar, N. (1993). Emplacement of nonaqueous liquids in the vadose zone. *Water Resources Research*, *29*(3), 705-722. doi:10.1029/92wr02450.

Parker, J. C., Kool, J. B. and Van Genuchten, M. T. (1985). Determining Soil Hydraulic Properties from One-step Outflow Experiments by Parameter Estimation: II. Experimental Studies 1. *Soil Science Society of America Journal*, 49(6), 1354-1359. doi:10.2136/sssaj1985.03615995004900060005x.

Parker, J. C., Lenhard, R. J., & Kuppusamy, T. (1987). A parametric model for constitutive properties governing multiphase flow in porous media. *Water Resources Research*, *23*(4), 618-624. doi:10.1029/wr023i004p00618.

Price, J. S., & Whittington, P. N. (2010). Water flow in Sphagnum hummocks: Mesocosm measurements and modelling. *Journal of Hydrology*, *381*(3-4), 333-340. doi:10.1016/j.jhydrol.2009.12.006.

Price, J. S., Whittington, P. N., Elrick, D. E., Strack, M., Brunet, N., & Faux, E. (2008). A Method to Determine Unsaturated Hydraulic Conductivity in Living and Undecomposed Moss. *Soil Science Society of America Journal*, 72(2), 487. doi:10.2136/sssaj2007.0111n.

Quinton, W. L., Elliot, T., Price, J. S., Rezanezhad, F., & Heck, R. (2009). Measuring physical and hydraulic properties of peat from X-ray tomography. *Geoderma*, *153*(1-2), 269-277. doi:10.1016/j.geoderma.2009.08.010.

Ramírez-Flores, J. C., Bachmann, J., & Marmur, A. (2010). Direct determination of contact angles of model soils in comparison with wettability characterization by capillary rise. *Journal of hydrology*, *382*(1-4), 10-19.

Rezanezhad, F., Quinton, W. L., Price, J. S., Elrick, D., Elliot, T. R., & Heck, R. J. (2009). Examining the effect of pore size distribution and shape on flow through unsaturated peat using computed tomography. *Hydrology and Earth System Sciences*, 13(10), 1993–2002. doi:10.5194/hess-13-1993-2009

Rezanezhad, F., Price, J. S., & Craig, J. R. (2012). The effects of dual porosity on transport and retardation in peat: A laboratory experiment. *Canadian Journal of Soil Science*, *92*(5), 723-732. doi:10.4141/cjss2011-050.

Sahni, A., Burger, J., & Blunt, M. (1998). Measurement of three phase relative permeability during gravity drainage using CT. In *SPE/DOE Improved Oil Recovery Symposium*. Society of Petroleum Engineers. doi:10.2118/39655-ms.

Schwärzel, K., Šimůnek, J., Stoffregen, H., Wessolek, G., & Van Genuchten, M. T. (2006). Estimation of the unsaturated hydraulic conductivity of peat soils. *Vadose Zone Journal*, *5*(2), 628-640.

Sigmund, P. M. & McCaffery, F. G. (1979). An Improved Unsteady-State Procedure for Determining the Relative-Permeability Characteristics of Heterogeneous Porous Media (includes associated papers 8028 and 8777). *Society of Petroleum Engineers Journal*, 19(01), 15–28. doi:10.2118/6720-pa.

Sohrabi, M., Henderson, G. D., Tehrani, D. H., & Danesh, A. (2000). Visualisation of Oil Recovery by Water Alternating Gas (WAG) Injection Using High Pressure Micromodels - Water-Wet System. SPE Annual Technical Conference and Exhibition. doi:10.2118/63000-ms.

Thomson, N. R., Graham, D. N., & Farquhar, G. J. (1992). One-dimensional immiscible displacement experiments. *Journal of contaminant hydrology*, *10*(3), 197-223.doi:10.1016/0169-7722(92)90061-i.

Van Geel, P. J., & Roy, S. D. (2002). A proposed model to include a residual NAPL saturation in a hysteretic capillary pressure–saturation relationship. *Journal of contaminant hydrology*, *58*(1-2), 79-110. doi:10.1016/s0169-7722(02)00012-8.

Van Geel, P. J., & Sykes, J. F. (1994). Laboratory and model simulations of a LNAPL spill in a variably-saturated sand, 1. Laboratory experiment and image analysis techniques. *Journal of Contaminant Hydrology*, *17*(1), 1-25. doi:10.1016/0169-7722(94)90075-2.

Van Genuchten, M. T. (1980). A closed-form equation for predicting the hydraulic conductivity of unsaturated soils 1. *Soil science society of America journal*, *44*(5), 892-898.

Highlights

- Water-NAPL relative permeability relations obtained for the first time in peat soil
- Water- & NAPL-air contact angle used to scale pressure-saturation relation in peat
- Peat bulk density increases residual NAPL/water saturation, decreases permeability
- Excavating ditches around the NAPL plume could effectively recover spilled NAPL